CANOPY REFLECTANCE MODELING IN A TROPICAL WOODED GRASSLAND

Principal Investigator: David Simonett, Professor of Geography

Department of Geography, University of California, Santa Barbara, CA 93106

Final Report, Year 1

NASA Award NAGW-788

1986

Report prepared by **Janet Franklin**

CANOPY REFLECTANCE MODELING IN A TROPICAL WOODED GRASSLAND

(*Report prepared by Janet Franklin*)

Final Report, Year 1, NASA Award NAGW-788

ABSTRACT

We are using geometric/optical canopy reflectance modeling and spatial/spectral pattern recognition to study the form and structure of savanna in West Africa. We are testing an invertible plant canopy reflectance model for its ability to estimate the amount of woody vegetation from remotely sensed data in areas of sparsely wooded grassland.

Dry woodlands and wooded grasslands, commonly referred to as savannas, are important ecologically and economically in Africa, and cover approximately forty percent of the continent by some estimates. The Sahelian and Sudanian savanna make up the important and sensitive transition zone between the tropical forests and the arid Saharan region. The depletion of woody cover, which is used for fodder and fuel in these regions, has become a very severe problem for the people living there. We are using Landsat Thematic Mapper (TM) data to stratify woodland and wooded grassland into areas of relatively homogeneous canopy cover, and then applying an invertible forest canopy reflectance model to estimate directly the height and spacing of the trees in the stands. Because height and spacing are proportional to biomass in some cases, a successful application of the segmentation/modeling techniques will allow direct estimation of tree biomass, as well as cover density, over significant areas of these valuable and sensitive ecosystems.

The model is being tested in sites in two different bioclimatic zones in Mali, West Africa. will be used for testing the canopy model. Sudanian zone crop/woodland test sites were located in the Region of Ségou, Mali.

Table of Contents

CANOPY REFLECTANCE MODELING IN A TROPICAL WOODED GRASSLAND

(*Report prepared by Janet Franklin*)

Final Report, Year 1, NASA Award NAGW-788

1. INTRODUCTION

> About noon we saw at a distance the capital of Kaarta, situated in the middle of an open plain — the country for two miles around being cleared of wood by the great consumption of that article for building and fuel...[February 11, 1796] (Park 1893)

The need for accurate baseline data on the type and condition of landcover for large areas of the earth has been recognized by many leading scientists (NASA 1983, Houghton et al. 1983, Woodwell 1984). Terrestrial biota greatly affect the climate, energy budget, hydrologic cycle and biogeochemistry of the Earth, and are in turn affected by these processes. Quantifying the effects of human impact on the biosphere requires a greatly improved understanding of the influence of human-induced changes in land cover (such as deforestation, "desertification," and conversion of land to agricultural and urban uses) on the spatial and temporal dynamics of terrestrial vegetation. This understanding may in turn help resource planners improve land use practices in areas where degradation of range and farmland and loss of fuelwood contributes to problems of hunger and disease. Global land-cover information is traditionally derived from small-scale vegetation maps and FAO statistics, and more recently from satellite imagery (Tucker et al. 1985, Justice et al. 1985, Matthews 1983). These estimates vary considerably, due to lack of consistency between data sources, particularly concerning classification and methodology (Ajtay et al. 1979, Matthews 1983).

Degradation of arid and semi-arid ecosystems has accelerated in recent years due to increased human use for fuel and food production, coupled with climatic fluctuation. Degradation is defined as a reduction in perennial phytomass and ecosystem productivity, elimination of woody cover, soil exposure, compaction, and erosion, and loss of stored nutrients and carbon (Dregne 1983, Petrov 1976, Vinogradov 1980, Reining 1978, and Hare 1983). This has occurred in sub-Saharan Africa, particularly the Sahel, in the last two decades. Mungo Park's remarks about the

kingdom of Ségu (now Mali) in the quote that opens this introduction demonstrate that deforestation is not a new problem (Park 1893), but now, for the first time in history, drought and famine are the focus of international media attention.

Several feedback mechanisms for prolonging droughts and accelerating land degradation have been proposed which involve land cover change. Because rain is primarily of convective origin in the tropics and subtropics, the source of the water either being the ground itself or a neighboring ocean, once a drought begins, the vegetation dies, reducing evapotranspiration and convective rainfall even further. Another feedback model states that the loss of vegetation causes increased surface albedo, drastically changing the energy balance of the surface, resulting in further drying (Charney 1975). However, in many parts of the Sahel zone the surface albedo again decreased after the drought period in the early 1970's (Rasool et al. 1982), implying that a runaway process of perpetuating the drought through increased surface albedo did not occur. Changes in evapotranspiration may be a more significant factor in perpetuating droughts (Rasool 1983). Therefore, changes in the amount of woody vegetation should be examined.

In the development of remote sensing techniques for vegetation assessment, the spectral vegetation indices and transforms that have been applied successfully to estimate green vegetation amount in agricultural and grassland ecosystems do not work as well in forests and semi-arid woodlands, bush, and shrublands, because the bulk of the biomass is not green biomass but in the woody structures. Absorption and shadowing by woody parts and the amount of bare soil visible has a complicated effect on greenness measures. Thus, it is important to account for the ecosystem architecture. Further, the information classes in remotely sensed scenes of arborescent landscapes are composed of spectral mixtures of objects (such as trees, shrubs, grass, and soil) and form a mosaic at the scale of satellite sensor resolution.

We are testing a geometric/optical canopy reflectance model which exploits the canopy geometry in an inversion technique to predict tree size and density. This model is applied in a savanna ecosystem, an ecosystem of great importance in terms of global ecology and human utilization.

2. BACKGROUND

The main methods used for measuring vegetation amount, form, and structure from remotely sensed data are (1) spectral pattern recognition, including clustering, classification and labeling (Franklin *et al.* 1986), and (2) establishing correlative relationships between vegetation characteristics and satellite reflectance data. In spectral pattern recognition and image classification (Haralick and Fu 1983), cover classes are identified, and vegetation characteristics are associated with the classes through stratified sampling and measurement. Inference of vegetation parameters (biomass, chlorophyll absorption, moisture content, color and spectral signature) from remotely sensed data is discussed by Jensen (1983) and Curran (1980). In brief, the estimation of such parameters by correlation with band ratios and/or linear transforms usually relies on the contrast between the visible absorption and infrared reflectance of green vegetation. Woody vegetation amount (tree or shrub cover), where vegetation cover is incomplete (particularly in semi-arid and arid environments) is more strongly related to spectral brightness than any other spectral transform (Colwell 1981, Olsson 1984 and 1985, Logan and Strahler 1982, Pech *et al.* 1986). This effect has been modeled by Otterman (1984 and 1985).

Another method of inference in remote sensing is proportion estimation, treating the reflectance of a pixel as a linear composite of the reflectance of scene components weighted by their relative area within the pixel. This method has been used to estimate vegetation amount in canopies with incomplete cover (Richardson *et al.* 1975, Jackson *et al.* 1979, Heimes and Smith 1977, Graetz and Gentle 1982, Pech *et al.* 1986).

2.1. Plant Canopy Reflectance Modeling

In contrast to pattern recognition, where scene elements are mapped into information classes based on their radiance measures, or spectral indices, where a biophysical parameter is related empirically to (transformed) spectral data, in **reflectance modeling** reflectance is predicted as a function of the physical and optical properties of the scene elements. Plant canopy reflectance modeling will be defined as one way of treating mathematically the interaction of electromagnetic

radiation with "scene elements", where the scene element is a leaf (sub-element) or canopy (aggregate). The approaches used are radiative transfer theory in the visible and near-infrared wavelengths and the the energy balance equation in the thermal regime. The goal in plant canopy modeling is to predict the optical reflectance or emission as a function of intrinsic biophysical properties of the scene elements. If the canopy model can be *inverted*, then canopy characteristics can be inferred from measured reflectance.

Strahler *et al.* (1986) and Smith (1983) review canopy modeling from a remote sensing viewpoint; the plant stand is being viewed by a sensor measuring electromagnetic radiation, and the signal received at the sensor is a function of the intrinsic properties of the target (the plant stand) and the other elements in the scene (such as atmosphere, soil, shadowing as a function of sun-sensor-surface geometry, and stand density and homogeneity). The problem in reflectance modeling is separating reflectance due to intrinsic properties of the plant stand from extrinsic properties due to varying irradiance, or atmosphere.

Smith (1983, p. 87) states:

> [B]ecause of the large random component in radiation modeling, tractable models will include a statistical component . . . . When significant spatial variation occurs in the horizontal direction such that plane-parallel approximations to the scattering and emmissive terrain elements are no longer valid . . . the three-dimensional structure of terrain elements becomes important and leads to the casting of distinct shadows resulting from the macrostructure and morphology of the elements. For vegetation targets a merging of radiative transfer theory and geometric optics is evident.

The model that we will apply treats the stand statistically as a population of individual plants, and uses geometric optics to predict the shadowing from the plant canopy.

2.2. Inversion of Canopy Models

Canopy models can use two sources of information for inversion; angular variation in response (directional reflectance), and covariance statistics of estimated mixtures across pixels (Smith 1983). Goel et al. (1984), Goel and Thomas (1984a and b) and Goel and Strebel (1983) show how numerical nonlinear optimization techniques can be used to invert the Suits (1972) or SAILS (Verhoef and Bunnick 1976) type model to obtain leaf area from directional reflectance

measurements if the other parameters of the model are known (solar and viewing zenith, azimuth between solar and viewing direction, leaf inclination distribution, leaf hemispherical reflectance and transmittance, soil hemispherical reflectance, and fraction of incident diffused light). Goel and Deering (1985) do the same thing but predict five of the model parameters through inversion, holding only soil hemispherical reflectance and skylight constant. The success of inversion is limited by how well the model actually predicts reflectance for a given canopy (runs in the forward direction). In the papers cited above the inversion underestimates leaf area in the infrared wavelengths (the model overestimates reflectance) at low sun angle and for sparse canopies, because the model doesn't account for shadowing.

Inversion of these models in a remote sensing situation may not be practical because one either has to measure complete hemispherical reflectance (not very practical even from a multi-look angle sensor because of the number of measurements needed), or estimate spectral parameters, which are dependent on cover type and soil background (even among agricultural types), and diffuse light, which depends on atmospheric conditions. This technique couldn't be used unless the cover type and estimations of these parameters were already known, but could be useful in an agricultural monitoring scenario (Jackson 1984).

The plane-parallel models have been important in understanding radiative transfer in vegetation canopies, especially in describing the bidirectional reflectance distribution function (BRDF) of the canopy given certain properties of leaf area, angle and azimuth distribution, leaf and soil BRDF, and so forth. However, these models do not account for variation in reflectance as a function of spatially heterogeneous vegetation cover. If prediction of scene properties is the goal, these models do not adequately bridge the gap to the pattern recognition (indirect inference) techniques. The models which employ geometric optics better describe actual canopies, both agricultural and natural, because they incorporate canopy geometry and treat biological populations statistically.

The geometric-optical models use the second information source, covariance statistics of estimated mixtures across pixels, for inversion. This is more practical in a satellite remote sensing

situation, but still there are several scene and canopy parameters that must be measured or estimated.

2.3. Li-Strahler Canopy Models

Li and Strahler (1985; see also Li 1981, Li 1983) developed a family of invertible, deterministic canopy reflectance models for sparse pine forest (i. e., forest with a discontinuous canopy). These models are invertible because parameters of tree size and density can be directly calculated from remotely sensed reflectance values, given appropriate ground calibration. The models are essentially geometric in character, treating trees as solid objects on a contrasting background, and estimates the proportion of each pixel in green canopy, shadow, and understory. Using the simple model, Li and Strahler estimated height and density parameters to within ten percent of values obtained from air photos for pine stands in northern California, U.S.A. We have extend this simple model to fit the savannah environment. The reflectance of a pixel is modeled as a linear combination of scene components weighted by relative areas. Pixels from an area of homogeneous tree cover can be taken as replicate measurements of reflectance. Interpixel variance in reflectance comes from three sources:

— variations in the number of trees among pixels
— variation in tree size within and between pixels
— chance overlap of crown and shadow within a pixel.

The assumptions of the simple model, modified to fit the savannah tree form, are:

(1) tree shape can be approximated by a simple shape, a hemisphere on a stick, or some other form (see Figure 1),
(2) tree shape is uniform (independent of size), and size and density are uncorrelated,
(3) the crown, although hemispherical in shape, can be modeled as a flat Lambertian reflector which absorbs visible wavelengths differentially (i.e., is green), and casts a shadow,
(4) tree size (expressed as squared crown radius) is lognormally distributed with a fixed mean and variance and a known coefficient of variation (standard deviation divided by the mean),
(5) spatial pattern (distribution of the number of trees per pixel) can be described by a distribution function (e.g. Poisson, double Poisson) so that, again, even if the mean density is not known, the CV is (or the CD, coefficient of determination, variance divided by mean),
(6) the ground surface underlying the tree canopy (e. g., understory) has a signature which is distinctly different from that of tree crowns and shadow, and

(7) illumination is from a point source at infinite distance and at a known angle from the zenith.

The sensor model associated with the simple canopy model is based on the following assumptions:

(1) the output of the sensor is a digital image, consisting of brightness values averaged over the spatial extent of each grid cell,
(2) the sensor is multi-spectral, and
(3) the sensor is sufficiently for from the ground that view angle can be considered vertical and uniform over the imaged area.

The simple model can be thought of as including two steps. First is "proportion estimation," or calculating the proportions of understory, illuminated crown area, and shadow in each pixel. Because these proportions are a direct function of the number and size of trees that appear in a pixel (providing that neither the crowns intersect nor shadows overlap), they can be used to calculate a dimensionless parameter, NR^2, for the stand, where R^2 is the square of the average cone radius and N is the density of cones per unit area. The second step requires calculating the mean and variance of NR^2 values for all pixels within a stand, and using these values to estimate the mean size and spacing parameters for lognormal and Poisson models. Because inversion of the model to obtain tree height and spacing requires calculation of interpixel variance, a homogeneous timber stand of certain minimal area (perhaps twenty pixels) is needed. This version of the Li-Strahler model is referred to as the "simple variance-dependent model."

The accuracy of the simple variance-dependent model is limited by the overlapping of crowns and shadows, which becomes significant when canopy cover reaches a level of about thirty to forty percent, depending on the shape of the trees and their angle of illumination. A subsequent Li-Strahler model, the modified overlapping model, accounts for overlapping of shadows and intersection of crowns as density increases and trees are spaced increasingly close to each other, and can be inverted accurately for stands of up to 75% or greater crown closure, if the trees are not too small (Li and Strahler 1985).

2.3.1. Geometry of the Model

Figure 1 shows the geometry of a hemisphere on a stick illuminated at angle θ. The radius of the hemisphere is r, and h is the height to the base of the crown. Let r^2 be the square of the crown radius. Let $\gamma = \tan^{-1}(h/r)$. The illuminated crown, shadowed crown and shadowed ground projected to the sensor will have areas:

Crown: $\frac{\pi}{2} r^2(1 + \cos\theta)$

Shadowed Crown: $\frac{\pi}{2} r^2(1 - \cos\theta)$

If $h \tan\theta > 2r$

Shadowed Background:

$\frac{\pi}{2} r^2(1 + \frac{1}{\cos\theta})$ (large sun angle or tall narrow trees)

or if $h \tan\theta < 2r$

Shadowed Background:

$\frac{\pi}{2} r^2(1 + \frac{1}{\cos\theta}) - 2r^2(t - \frac{1}{2}\sin 2t)$ (small sun angle or short wide trees)

where $t = \cos^{-1}\frac{h\tan\theta}{2r} = \frac{\cos^{-1}\tan\theta}{2\tan\gamma}$.

In the original formulation, Li (1981) treated shadowed crown and background as one component, with a single signature, and the area calculated from tree geometry.

We will define Γ as the geometric factor, such that $\Gamma \sum_{i=1}^{n} r_i^2$ is the area of the pixel covered by tree and shadow. Therefore,

$$\Gamma = \pi + \frac{\pi}{2}(1 + \frac{1}{\cos\theta}) \quad \text{or,} \quad \Gamma = \pi + \frac{\pi}{2}(1 + \frac{1}{\cos\theta}) - 2r^2(t - \frac{1}{2}\sin 2t)$$

2.3.2. Variables and Notation

1) *Variables Associated with Tree Crowns:*

r Radius of crown as hemisphere, lognormally distributed.

h Height to base of crown, lognormally distributed. Crown height, $H = r + h$.

C_r Coefficient of variation of crown radius.

2) *Variables Associated with a Pixel:*

A Pixel size. Usually taken as having a unit area.

n Number of trees in a pixel, distributed as a Poisson; independent of other variables.

R^2 Average of squared crown radii within the pixel, i.e., $R^2 = \frac{1}{n}\sum_{i=1}^{n} r^2_i$.

m Dimensionless. Ratio of sum of squared crown radii to area of pixel, which is

$$m = \frac{nR^2}{A} = \sum_{i=1}^{n} r_i^2/A.$$

Note that m is a dimensionless parameter reflecting both the size and density of trees and $m\pi$ is the proportion of crown closure in the stand. The larger m, the larger or denser the trees. This is scaled by the geometric factor, Γ, to get the proportion of pixel in canopy, shadow and background.

3) *Variables Associated with the Woodland Stand:*

N Mean of n for all pixels. For the random model, this is the value of the Poisson parameter.

D_n Dispersion coefficient (variance-to-mean ratio) of n. That is, $D_n = V(n)/N$. If n is distributed as a Poisson function, $D_n \approx 1$. If not, D_n will depend on the pixel size, A. For the clumped or patchy distributions that characterize large quadrats in natural forests, D_n will increase with A.

$E(r)$ Population mean of r.

$V(r)$ Population variance of r. $V(r) = C_r^2 (E^2(r))^2$.

$E(r^2)$ Population mean of r^2.

$V(r^2)$ Population variance of r^2.

$CR\,2$ Coefficient of variation of squared crown radius for the stand.

If r is lognormally distributed, then r^2 is also lognormally distributed. We can then show from the definitions of E and V that

$$E(r^2) = (1+C_r^2)E(r)^2,$$

and

$$V(r^2) = w\,[E(r^2)]^2\,,$$

where

$$w = (1+C_r{}^2)^4 - 1.$$

$\mathbf{R}^2$ Mean value of R^2 for all pixels. i.e., $E(R^2)$.
$\mathbf{R}$ The square root of $\mathbf{R}^2$, i.e., $\sqrt{E(R^2)}$.
$V(R^2)$ Variance of R^2.

If n is a constant and r is randomly distributed in the spatial domain, then $\mathbf{R}^2 \approx E(r^2)$. Also, R^2 is a sample mean, and thus $V(R^2) = V(r^2)/n$.

M Mean of m for all pixels in the stand.
$V(m)$ Variance of m.

2.3.3. Reflectance of an Individual Pixel

As stated above, we model the reflectance of the pixel as an area-weighted sum of the reflectances of the four spectral scene components.

1) *Areas and Proportions:* Next are variables describing areas or proportions for scene components.

A_g Area of illuminated background within the pixel.
A_c Area of illuminated crown within a pixel.
A_z Area of shadowed background within a pixel.
A_t Area of shadowed crown within a pixel.
K_g $=A_g/A$ Proportion of pixel not covered by crown or shadow.
K_c $=A_c/(A-A_g)$ Proportion of area covered by crown and shadow that is in illuminated crown.
K_t $=A_t/(A-A_g)$ Proportion of covered area in shadowed crown.
K_z $=A_z/(A-A_g)$ Proportion of covered area in shadowed background.

From the tree geometry described above, we can show that

$$A_c = m\,\frac{\pi}{2}(1+\cos\theta)$$

$$A_t = m \frac{\pi}{2}(1 - \cos\theta)$$

$$A_z = m \frac{\pi}{2}(1 + \frac{1}{\cos\theta}) \text{ if } h\tan\theta < 2R$$

or

$$A_z = m \frac{\pi}{2}(1 + \frac{1}{\cos}\theta) - 2r^2(t - \tfrac{1}{2}\sin 2t) \text{ if } h\tan\theta > 2R .$$

So,

$$A_c + A_t + A_z = m\Gamma$$

and

$$A_g = 1 - m\Gamma.$$

2) *Reflectance Vectors:* These are average single channel reflectances or multispectral reflectance vectors.

G Reflectance vector for a unit area of illuminated background (constant).
C Reflectance of a unit area of illuminated crown (constant).
Z Reflectance of a unit area of shadowed background (constant).
T Reflectance of a unit area of shadowed crown (constant).
S Reflectance of a pixel. Variable; depends on number and size of trees in pixel.
$V(S)$

The signature of pixel i in band j (for single channel, drop the subscript j) is

$$S_{ij} = (G_j \cdot A_g + C_j \cdot A_c + Z_j \cdot A_z + T_j \cdot A_t)/A \quad (1)$$

3) *Geometric Relationships:* From the geometry of the hemisphere, we have the following relations if the pixel is taken to have a unit area:

$$(A - A_g) = \sum^{i} r_i^2 \Gamma = Am\Gamma$$

$$(A - A_g) = A_c + A_t + A_z$$

$$K_g = 1 - m\Gamma$$

$$K_c = (\frac{\pi}{2}(1 + \cos\theta))/\Gamma$$

$$K_z = (\frac{\pi}{2}(1 + \frac{1}{\cos\theta}))/\Gamma$$

$$K_t = (\frac{\pi}{2}(1 - \cos\theta))/\Gamma$$

$$1 = K_c + K_z + K_t \ .$$

Equation (1) can be formulated:

$$S = K_g \cdot G + (1-K_g)\cdot(K_c \cdot C + K_z \cdot Z + K_t \cdot T) \ . \tag{2}$$

Since K_c , K_z , and K_t sum to one, the expression $(K_c \cdot C + K_z \cdot Z + K_t \cdot T)$ represents a point in multispectral space lying within a triangle with vertices at C , Z , and T (see Figure 2). This point is X_0 ; the average reflectance of a tree and its associated shadow. The only variable in the right side of (2) is thus K_g , which is a linear function of m . When m varies, S will vary along a straight line connecting points G and X_0.

Note that as overlapping of trees and shadows occurs, the background is obscured and shadows falling on other crowns will be foreshortened. Therefore, the reflectance of a pixel that is all tree and shadow, X_∞, will lie on line TC , its position depending on tree geometry and sun angle.

Substituting the geometric expressions above for K_c , K_z , and K_t into (2) yields

$$S = (G - Gm\Gamma) + X_0 m\Gamma \ .$$

Rearranging, we have

$$m\Gamma(G - X_0) = (G - S) \ . \tag{3}$$

In the last expression, $G-S$ and $G-X_0$ are vector differences; however, $G-S$ lies on the line $G-X_0$ and therefore the equation is actually scalar. Using the notation $|GS$ to indicate the length of the vector connecting G and S , we have

$$m = \frac{|GS}{\Gamma|GX_0} \tag{4}$$

If there were no error in the signal, the m value determined in any band would be the same, but noise will be present in S, α, and the component signatures. Two averaging procedures can be used; the weighted average of m values for all bands, or the weighted average of the final estimates of height and spacing. In the single band case, the outliers will inflate the variance more, making the trees appear bigger.

The sensitivity of this model to noise in S and the component signatures, and to errors in estimation of parameters can be shown by taking the partial derivative of m with respect to these variables. Rearranging and expanding (3) we get

$$m = \frac{G}{\Gamma(G - X_0)} - \frac{S}{\Gamma(G - X_0)} = \frac{G}{\Gamma(G - X_0)} - \frac{1}{\Gamma(G - X_0)} \cdot S \tag{5}$$

and from this,

$$\frac{\partial m}{\partial S} = \frac{1}{\Gamma(G - X_0)} \tag{6}$$

$$\frac{\partial m}{\partial G} = \frac{S - X_0}{\Gamma(G - X_0)^2} \approx \frac{1}{\Gamma(G - X_0)} \tag{7}$$

(because when cover is low, $S \approx G$)

$$\frac{\partial m}{\partial X_0} = \frac{G - S}{\Gamma(G - X_0)^2} \approx \frac{m}{G - X_0} \tag{8}$$

$$\frac{\partial m}{\partial \Gamma} = \frac{S - G}{\Gamma^2(G - X_0)} \approx \frac{m}{\Gamma} \tag{9}$$

Because $(G - X_0)$ is in the denominator, when the spectral contract between background and tree is high, sensitivity to noise in S, G and X_0 will be reduced. When density is low (m is small), noise or error in estimating X_0 and Γ are less important than the contrast between tree and background $(G - X_0)$, because m is in the numerator.

2.3.4. Inverting the Model using the Variance of m

Assume that a woodland stand consists of K pixels, $i=1, \ldots, K$. From (2), we can obtain a value of m for each pixel. Then, the values of m will have a mean and a variance within the timber stand:

$$M = \frac{1}{K}\sum_{i=1}^{K} n_i R_i^{\,2} ;$$

$$V(m) = \frac{1}{K}\sum_{i=1}^{K} (n_i R_i^{\,2} - M)^2 .$$

Let us now assume that height (and thus r) is independent of density. Thus, expressions for the mean and variance of independent products will apply:

$$M = E(nR^2) = E(n) \cdot E(r^2) = N\mathbf{R}^2 , \tag{10}$$

and

$$V(m) = V(nR^2) = (\mathbf{R}^2)^2\, V(n) + N^2 V(R^2) + V(n)V(R^2) . \tag{11}$$

Because n is a Poisson function,

$$V(n) = N . \tag{12}$$

Further,

$$V(R^2) = V(r^2)/n \approx V(r^2)/N = w\,(E(r^2))^2/N . \tag{13}$$

Substituting (12) and (13) into (11), we finally obtain:

$$V(m) \approx (N + CR\,2N + CR\,2)(\mathbf{R}^2)^2 = (M + CR\,2M + CR\,2\mathbf{R}^2)\mathbf{R}^2 . \tag{14}$$

In order to derive (14), $\mathbf{R}^2$ and $V(R^2)$, which are parametric terms, are approximated using the sample mean and variance of r^2. Small errors are introduced by these approximations, but they

may be ignored for our purposes. Solving (14) for $\mathbf{R}^2$, we obtain:

$$\mathbf{R}^2 = \frac{[(1 + CR\,2)^2 M^2 + 4V(m)CR\,2]^{1/2} - (1 + CR\,2)M}{2CR\,2} . \tag{15}$$

Thus, given sample estimates of the mean and variance of M determined from the reflectances of pixels in the stand, we can solve for $\mathbf{R}^2$, and then for N, yielding the average size and density of trees in the stand. The assumption underlying the use of the sample variance of r^2 as $V(R^2)$ is that each pixel is an independent sample of values of r^2. Other approximations can be also applied to (11). For example, if the interpixel variation of r^2 is more significant than intrapixel variation, we may use $V(R^2)$ directly as an approximation of $V(r^2)$. Then (14) becomes:

$$V(m) = (1 + CR\,2)M\mathbf{R}^2 + CR\,2M^2$$

and we obtain:

$$\mathbf{R}^2 = \frac{V(m) - CR\,2M^2}{(1 + CR\,2)M} . \tag{16}$$

Also, if the dispersion coefficient of n is significantly different from 1, we may use $V(n) = ND_n$. Then (15) becomes:

$$\mathbf{R}^2 = \frac{((D_n + CR\,2)^2 M^2 + 4V(m)\ CR\,2D_n)^{1/2} - (D_n + CR\,2)M}{2CR\,2D_n} . \tag{17}$$

The choices basically depend upon what *à priori* information we have (Li and Strahler 1985).

3. STUDY AREA

3.1. The Savanna Biome

The study is being conducted in the Sahelian and Sudanian zone savannas of West Africa. Dry woodlands and wooded savanna (with tree cover greater than 10%) are presently estimated to cover 486.4 million ha or 22.2% of the continent of Africa, including 8.6 million ha in Mali (Lanley and Clement 1982). Savanna will be defined as the subtropical and tropical vegetation formations where the grass stratum is continuous and important, occasionally interrupted by trees and shrubs (cover greater than 10% and less than 80%), where fire occurs, and where the growth is closely associated with alternating wet and dry seasons. The savanna forms the broad transition between closed tropical forest and open desertic steppes (Bourlière and Hadley 1983).

Because of the difficulties in estimating changes in savanna and dry woodland area using available monitoring techniques, the most authoritative study declines to estimate changes in these categories (Lanley and Clement 1982). However, the rate of conversion to other vegetation types by clearing for agriculture, grazing, burning and fuelwood harvesting appears to be very high. For example, in Tanzania, miombo and other dry woodlands in populated areas are being harvested more rapidly than they can regenerate (Allen 1983). The problem in drier savanna in the Sahel may be even more severe (Delwaulle 1973).

The balance between woody and herbaceous plants, and the effects of various factors on this balance is one of the most interesting aspects of the dynamics of savanna ecosystems (Bourlière and Hadley 1983, Lebrun 1955). Walker and Noy-Meir (1982) have proposed a model of savanna structure based on the idea of dynamic equilibrium, which assumes that the strata compete for topsoil water, and an increase in tree leaf biomass must be balanced by a decrease in herbaceous biomass (shown empirically in the Sahel by Breman 1982). Although the strata are in competition for soil moisture, the woody strata also create favorable microhabitat for herbaceous growth. The recovery of herbaceous vegetation after the 1972-73 drought in the Sahel was quicker where woody vegetation was present (Bernhardt-Reversat 1977). Walker and Noy-Meir conclude that

savanna is perturbed by climatic shifts, fire, grazing, and fuelwood consumption, which is reflected in the changes in relative proportions of grass and trees. However, theories on the mechanisms controlling savanna structure are hotly debated (Menaut 1983). The savanna structure, particularly the proportion of woody cover, is an important indicator of environmental conditions. Our canopy model will provide a method for measuring woody cover over large areas.

3.2. Savanna Vegetation of West Africa

The rainfall gradient is very steep in tropical and sub-tropical West Africa, about 1 mm/km latitude, and the rainy season is unimodal. The savanna bioclimatic regions are referred to as the Sahelian and Sudanian zones. This region is a vast plain, interrupted by some escarpments and massifs, but mostly composed of eroded sedimentary material and Pleistocene fossil dune systems. The plain is often internally drained into small depressions, and throughout the region there is an impermeable (often ferricrete) layer at varying depth and of varying thickness. These features control the local distribution of vegetation.

Sahel is an Arabic word meaning shoreline, and refers to the southern boundary of the Sahara desert. The Sahelian zone corresponds roughly to the 200-400 mm annual precipitation zone, and is further subdivided into:

Saharo-Sahelian transition	100-200 mm
Sahel proper	200-400 mm
Sudano-Sahelian transition	400-600 mm

by Chevallier (1900), Aubréville (1949), Boudet (1975), Le Houerou (1980), Penning de Vries an Djiteye (1982), and Breman and de Wit (1983). The rainy season varies from 1.5 mos in the north to 3.5 in the south, from 20 rain days to 60, and the mean annual precipitation coefficient of variation ranges from 40 % to 25% (Tucker *et al.* 1985). The vegetation of the Sahel ranges from an open annual grassland (*Panicum turgidum, Cenchrus biflorus*), with less than 10% woody cover dominated by spiny trees and shrubs (*Acacia raddiana, Balanites aegyptica, Zizyphus*

mauritanica), in the north to perennial grasses with 25% or more tree cover (including Combretaceae — *Combretum, Terminalia*) in the south. The northern limit of the Sahel is sometimes defined by the absence of the grass *Cenchrus biflorus* ("kram-kram"). Basal area ranges from 4-16 m^2/ha for the tree layer (Rutherford 1982), and annual production by woody plants of leaves, stems and twigs is 80-300 kg/ha/yr (Le Houerou 1980). The latitudinal trend in density of woody cover is modulated by topographic position and soil type (affecting moisture availability). For example, *Acacia nilotica* and *A. seyal* are locally dominant and dense in low, flooded areas, *Euphorbia balsamifera* is dominant in the northern Sahel where the impermeable ferricrust is close to the surface, and shallow gravelly slopes have a unique floristic association (the "Brousse tigré").

Leaf biomass can be predicted from stem circumference, tree height, or crown diameter ($R^2 \approx .80$–$.96$) (Cissé 1980a and b, Bille 1980). In the Sahel, green leaf biomass of woody species, and crown closure were shown to be proportional to mean annual rainfall and inversely proportional to herb cover (Cissé and Breman 1982). A study in the Sudan showed a strong correlation (R=.94) between woody biomass and crown diameter (Olsson 1984). Since the canopy model predicts average crown size and density, this bodes well for using the model to estimate biomass.

Phenology of trees and grasses is highly variable, and dependent of species and morphological differences, the presence of deep soil water, and so forth. However, many woody plants in the Sahel leaf out at the end of the wet season, greening up as much as three months after the peak of herbaceous productivity (for example, *Acacia senegal, Commiphora africana, Combretum micranthum, Euphorbia balsamifera, Guiera senegalensis* and *Zizyphus mauritiana;* Poupon and Bille 1974). Other species have the opposite pattern, greening in the late dry season before the rains.

The *Sudanian* zone is the region to the south of the Sahel, lying between about 11° and 13° N in West Africa, where the rainfall is 600 to 1000 mm, the rainy season lasts 4 to 5 months, and there is permanent agriculture. The vegetation is a mosaic of open woodland savanna, up to about 15 m tall, some closed woodland, and edaphic bush thickets and grasslands on ferricrete

and inundated soils. Dominant woody species include *Vitellaria paradoxa, Acacia albida, Albizia chevallieri, Prosopis africana, Cassia seiberiana, Adansonia digitata* and *Parkia biglobosa.* The northern limit of the Sudanian zone is marked by the disappearance of *Vitillaria paradoxa* ("karité"), and *Adansonia digitata* (baobab) (Schnell 1977). This zone has been cultivated for a long time, with areas near villages under permanent cultivation, and bush fallowing practiced in fields further away. The crop/woodland or "orchard bush" type of vegetation is formed when crops are grown under a woodland of useful trees which are preserved when the land is cleared (Nielsen 1965).

All of these characteristics (open tree canopy, herbaceous understory, simple basal area/-biomass relationship, woodland of continuously varying density, but complex spatial mosaic of physiognomic types) indicate that the stratification approach and the Strahler-Li canopy model will be applicable to this area, and provide a method for assessing woodland structure, and detecting and quantifying woody cover.

3.3. Sahelian Sites in Mali

A study is being conducted in the Gourma area of Mali by the Centre International pour l'Elevage en Afrique (CIPEA; Pierre Hiernaux, Principal Investigator), in collaboration with the GIMMS (Global Inventory, Monitoring and Modeling System) Project at NASA/Goddard Space Flight Center. CIPEA has located thirty sites of one kilometer radius along a north-south transect from near Douna in the south (14° 40′ N, 1° 35′ W, 500 mm annual ppt.), to Gourma-Rharous on the Niger River in the north (17° 45′ N, 1° 50′ W, 250 mm annual ppt.). These sites were chosen to be of relatively homogeneous vegetation and substrate (according to tone and texture on air photos) over and area of at least one square kilometer, for an AVHRR study (Hiernaux and Justice 1986).

In the first year we are testing the canopy model in CIPEA Sites 15 (near Gossi), 20 and 21 (near Hombori — see Figure 3). Site 15 is located in an *Acacia nilotica* woodland (approximately thirty percent cover), with an understory of predominantly *Echinochloa colonna* on an alluvial

plain of poorly drained vertisols. Part of this stand can remain flooded throughout the dry season (Hiernaux *et al.* 1984). Site 20 is located in an *Acacia seyal* woodland (approximately fifty-seven percent cover), with forty-seven percent herbaceous cover (*Echinochloa, Sporobolis helvolis,* and *Corchorus tridens*), also on an alluvial plain of vertisols, that is inundated during the rainy season, but more freely drained that Site 15 (Hiernaux et al. 1984). Site 21 is very similar to Site 20, with woody cover approximately fourty-four percent, predominantly *Acacia seyal* (personal observation and P. Hiernaux 1985, unpublished data).

3.4. Sudanian Sites in Mali

The Sudanian test sites are in the Region of Ségou, between Tamani and Konodimini (6° 50′ W and 6° 20′ W) and the Niger River and Nango (13° 25′ N and 13° 10′ N). This area is being used by R. Cole (Department of Geography, Michigan State University), in his study of the changes in land use practices in response to the drought since the early 1970's. Rainfed crops are grown during the two to three month growing season under a canopy of useful trees which are preserved when the land is cleared for planting (predominantly *Vitellaria paradoxa, Acacia albida, Adansonia digitata, Ficus sp., Tamarindus indica,* and *Parkia biglobosa).* In November 1985 measurements were taken at four sites in the Region of Ségou (Figure 4). Sites 1 and 2 are dominated by *Vitellaria paradoxa,* and are located southwest and east of Konodimini respectively, in the house fields (cultivated areas near the village where shrubs and weeds are cleared regularly). Sites 3 and 4 are dominated by *Acacia albida,* and are located in the house fields surrounding the villages of Massala and Dugufé. *Acacia albida* has a characteristic distribution pattern in this area. Preserved near villages, it dominates within a distance of 0.5 km of the village perimeter with crops grown beneath. Beyond that distance, karité dominates where there is cultivation.

3.5. Image and Collateral Data

Thematic Mapper data for the study areas have been acquired. Geometrically corrected P-Tapes were purchased from EOSAT. For the Gourma test sites a scene was chosen from the late part of the growing season (9 September 1984). The scene is #5019209552, WRS Path 195, Row 49 (Quadrant 3), which includes the sites from north of Gossi to south of Hombori (Sites 14 to 21 and 31, see Figure 3). This date was chosen because it coincided with CIPEA field data collection. However, this scene is not optimal for discriminating trees from herbaceous understory, because there were several September rainfall events in 1984, and in this image the herbaceous vegetation is still green in the wetter sites (e.g., Site 15) and in some areas of the dunes. Therefore, a late dry season image (7 May 1985) has been acquired, to use for multi-date stratification, and for testing the canopy model in contrasting seasons. For the Region of Ségou, a post-harvest, early dry season image (17 November 1984) was acquired (Scene #5026110142, Path 198, Row 51).

Topographic maps at several scales (1:200,000 and 1:1,000,000) were acquired for both the Gourma and Ségou sites. Black and white aerial photographs are available for the Republic of Mali at a scale of 1:60,000, but they date from 1956. These are the only small-scale photographs available in the Gourma area, and are required for image registration, location of study sites, strata labeling, and so forth. Therefore, partial coverage for the Gourma area was acquired. In the Region of Ségou, 1:50,000 black and white panchromatic photos from 1974 are available for part of the region due to the presence of "Projet Riz" (an extensive irrigation project for rice growing) in this area. These photos have been purchased. Current (1985-1986) low-level color air photos (1:2500 to 1:5000 scale) for some of the study sites in both regions were made available to us by CIPEA. All of these maps and photo data sources are used for locating study sites, model parameterization (calculating tree spatial pattern and measuring density and cover for sample stands to be used in accuracy assessment), image registration (to help interpret from satellite imagery to topographic maps) and strata labeling during the image stratification step.

4. METHODS

4.1. Pattern Analysis

The purpose of pattern analysis is to to explore the temporal and spatial patterns of the imagery and the ground scene in order to guide the choice of stratification techniques. Recent work (Woodcock and Strahler 1983, Woodcock 1986) shows that spatial pattern in multi-spectral scanner imagery is dependent on scale, and the spatial characteristics of the scene elements within a particular information class or cover type. Two-dimensional variograms will be calculated (see Woodcock 1986) for test areas of different known vegetation types in the image data. The expected result is a description of the spatial variance of tones in the images, which will indicate the relative scales of pattern, and provide a basis for choosing an appropriate texture measure, or describing the image context function, for possible use in the segmentation step.

Many researchers have attempted to understand and describe the pattern of vegetation in the woodland/grassland/shrubland complex of west Africa and there is no simple deterministic model of the spatial and temporal distribution of vegetation in this or any area with a long and complex land use history. However, it may be possible to include information about vegetation spatial pattern in the information extraction process, at least empirically.

4.2. Image Stratification

The purpose of image stratification (or segmentation) is to identify areas of woodland in the image, and stratify the area into woodland stands of some minimum area which are of relatively homogeneous density. This task has been successfully accomplished in prior research (Franklin et al. 1985, Strahler et al. 1983) by using MSS, image texture and digital terrain data, carrying out unsupervised classification, then subsequently performing spatial filtering to produce spatially homogeneous stands.

For the present study terrain data will not be used. It is not available, and would be marginally useful in this environment for discriminating vegetation types. We will use two-date TM

imagery (one wet season and one dry season image), and possibly a texture image (Zhan 1986) as input to unsupervised classification. Principal components images, either from each date, or both dates combined, could be used to reduce the number of data channels used in classification. We anticipate that with two-date, well-registered images, the cover types can be discriminated spectrally, possibly with the help of a texture measure. The classification will be evaluated using standard accuracy assessment procedures for thematic maps (Rosenfeld *et al.* 1982, Card 1982), and by the ability of the stratification to reduce variance in cover estimates or basal area within woodland strata. Note that in the Gourma study site, a vegetation stratification identifying soil- and woody cover classes can also be used by Hiernaux and Justice to improve biomass estimates using NDVI from aircraft radiometer or AVHRR data (Hiernaux et al. 1986).

4.3. Canopy Reflectance Modeling

The tree cover in savanna wooded grassland is sufficiently sparse that the overlapping of shadows and crowns should not be a significant problem and the simple variance dependent model can be applied. The following assumptions were modified from those used in the simple Strahler-Li model:

(1) **tree shape**: A hemisphere on a stick model for tree shape is appropriate for Saheliant and Sudanian savannas. Li and Strahler have extended the model for this shape (Figure 1). The ratio of height to crown diameter was established from test data.

(2) **size distribution**: Field measurement of size distribution are very important in the Sahelian and Sudanian zones where extensive measurements of these parameters do not exist. We measured size distribution in all of our field sites.

(3) **spatial distribution**: Our earlier research (Strahler and Li 1981, Franklin 1983) has shown that it is possible to estimate the spacing parameters of the model from medium-scale air photos. Spatial pattern was alos sampled from air photos for our Mali sites.

(4) **component spectral signatures**: Sensitivity analysis of the Li-Strahler model shows that the larger the difference between the Background and Tree-Shadow signatures, the stabler the

results. If a projection can be chosen in spectral space which maximizes spectral separability of the components, this will minimize error. Also, as each tree has a bigger impact (as the sun angle, and therefore the amount of shadow increases) the results are more stable. When trees are small or sparse, the above factors are more important than noise in the tree signature, or in the shape parameter. This makes intuitive sense — when the amount of "treeness" in the pixel is low, the model is more sensitive to variations in the background signal than the tree signal.

Therefore, the natural variability of the tree population in terms of shape and spectral properties, will not cause significant errors on the model results, but variations in the background signature will. A band combination or projection in spectral space can be chosen which minimizes variations in background signature.

(5) **tree size and density for test stands:** In order to verify model results, tree size and density were sampled in test stands.

4.4. Field Data Collection 1985

In the Gourma sites the CIPEA team has estimated woody cover by the line intercept method, and estimated tree height, circumference, and crown area for the trees intercepted by the one kilometer transect. We have received the tree cover and dimensional data from CIPEA so that the distribution of tree sizes can be established for the sites, and cover estimates can be used to verify model results. Also, in an earlier study (Cissé 1980b) stratified (by diameter class) samples of several dominant Sahelian woody plants were measured to establish the dimensional relationships among height, stem diameter and crown diameter. These data were used to establish the shape parameter (h/R) for the model.

In the Ségou region, four 50 to 60 m radius plots were located in each of the four sample stands. Diameter at breast height (dbh) of each tree, and height and shape parameters for a subsample of the trees (16 trees per plot) were measured. From these measurements the shape parameter and the size distribution for the stands were estimated.

4.5. Analysis of Aerial Photographs

Using the low altitude CIPEA photographs of the training sites, we have mapped tree point pattern in two Gourma and two Ségou sites. In 280 x 280 m, 250 x 250 m or 140 x 140 m quadrats 200 to 900 trees per quadrat were located. Spatial pattern has been analyzed using quadrat analysis (Li and Strahler 1981; Franklin et al. 1985, from Grieg-Smith 1964 and Pielou 1977), and second order analysis of inter-tree distances (Franklin and Getis 1985, Getis and Franklin 1986). We have also sampled density and tree cover for the quadrats by the dot grid method (Warren and Dunford 1983), to assess the accuracy of the model.

4.6. Image Processing

Principal Components Images: Principal components images were produced for each subimage separately from six TM spectral bands (not including the thermal channel because of the lower spatial resolution). Principal components images can be used as input to image stratification and canopy model testing (see below).

Image Stratification: The method used for image stratification is unsupervised clustering, classification, and cluster labeling. A small test area (256 x 256 pixels) was chosen in each subimage, and classification and clustering were performed both on principal components (PC) images and TM spectral bands. Spectral classes were inspected to determine if TM or PC images better discriminated the land cover classes in these areas.

Stand and Component Signatures: The mean and variance of the reflectance in each spectral band were computed for the test sites (these make up the vector S). The spectral signatures of the model components must also be calculated. Background signature were assigned from training sites. Tree plus associated shadow signature was estimated in two ways. For sites where there are cover measures in plots that can be located in the image, spectral brightness was regressed against cover, and extrapolate to 100 percent cover. For the other sites, unsupervised spectral clustering of the spectral data *within* the site was performed, assuming that the "darkest" class has the cover density measure by CIPEA. The co-spectral plot of red and near infrared

reflectance (or greenness and brightness) was inspected, and we assumed that brightness decreases and greenness increases linearly with cover.

Testing the Model

Model inversion was tested for single spectral bands. The parameters needed to calculate to test the simple model are the component signatures, G and X_0, the shape parameter α ($= r/h$), and $CV(R^2)$. The cosine of the solar zenith angle was calculated for each image based on the date and local time of the overpass, and the latitude and longitude of the scene center, using a program written by Jeff Dozier. The simple model was tested using programs written by Li Xiaowen.

5. RESULTS

5.1. Tree Shape and Allometry

The tree shape parameter for a hemisphere model, h/R, the ratio of stem height to crown width), was calculated empirically from sample data for each study site, and from other other studies, for five tree species (Tables 1 and 2). In this study each of these species dominated in the sites where they were found, making up over 80% of the crown cover. The shape parameter varies from 0.5 to 1.7, with most values falling between 0.7 and 1.5. From this shape parameter and the sun angle at the time of the Landsat overpass, Γ was calculated for input to the simple model (Table 3).

Table 4 shows the allometric relationships among crown radius (or diameter, or surface area), stem diameter (or circumference) and height. The R^2 values for the stratified (by size class) samples (from Cissé 1980 b) are improved over the values for the larger random samples (from Hiernaux *et al.* 1984 and this study) but are more representative of the predictive power of these relationships. The stratified sample more closely approximates a Model I regression (see Sokal and Rohlf 1969), where the independent variable is under investigator control.

5.2. Tree Size Distribution

Histograms of each of the sample populations were inspected to determine the shape of the size distributions. Histograms of crown size, height and stem size were examined, and because of the intercorrelation of these measurements (see last section) the shape of the distributions were similar. A lognormal distribution of tree size describes most of the sample populations. The distributions were right-skewed and a log transform of the data produced a normal looking distribution (Fig. 5). Therefore, a lognormal distribution can be accepted as describing the tree size distribution, and if CR 2 is not known from field data it can be calculated from the formula for a lognormal distribution. In this study CR@ was calculated from the field data (Table 2).

5.3. Spatial Pattern

Figure 6a shows the tree point locations for Gourma Site 20 as an example of the data set used to calculate spatial pattern. The results of second order analysis (Getis 1984, Franklin *et al.* 1985 and Getis and Franklin 1986) for sample quadrats in the test sites are as follows:

Gourma Site 20: (n = 895, 280 x 280 m quadrat) There is significant (at 1% level) inhibition (regular spacing) at 6 to 7 m distance, and significant (at 5% level) clumping at 30 to 100 m (Figure 6b), but the pattern looks very regular, and the clumping found by this method contradicts the results of the quadrat analysis (see below).

Gourma Site 15: (n = 589, 280 x 280 m quadrat) There is significant (at 1% level) inhibition at less than 5 m distance, and significant (at 5% level) clumping at 20 m and 100 m. At 25 to 80 m distance (satellite scanner resolution) the Poisson model (or Complete Spatial Randomness) is adequate (Fig. 7b).

Ségou Site 2: *Subplot 1:* (n = 222, 250 x 250 m quadrat) Inhibition to 8 m, Poisson model adequate from 9 to 50 m, significant aggregation from 60 to 100 m (at 1% level). *Subplot 2:* (n = 228, 250 x 250 m quadrat) Inhibition to 8 m, Poisson model fits from 10 to 26 m and 36 to 100 m, significant aggregation at 28 to 34 m (at 5% level) (Fig. 8).

Figure 7a shows the point locations for trees in Gourma Site 15 with a 30 m grid overlain, to illustrate how counts of trees would vary in TM-sized pixels. The results of variable sized quadrat analysis (Franklin *et al.* 1985) are shown in Table 5. Gourma Site 20 is fit by a Poisson model for quadrats of size 20 to 35 m, but not 40 m. This is partly a function of decreased sample size. Gourma Site 15 is fit by a Poisson model for quadrats of size 20 to 50 m, except that counts in 30 m quadrats differ significantly from Poisson. Ségou Site 2 (Subplot 1) is fit by a Poisson model for quadrats of size 10 to 60 m.

Our conclusion from these preliminary analyses of some of the sample sites is that a random (Poisson) spatial model is adequate at relevant sensor resolution of 20 to 50 m pixels. At coarser resolution, second order analysis shows the Poisson model to be adequate at distances of 50 to 100 m in most cases, including the sparser stands (Ségou Site 2) where our earlier studies show that

the Poisson model breaks down (Franklin *et al.* 1985).

5.4. Canopy Model

Results from the first test of the simple model are shown and described in Appendix A, which contains a paper presented at the Twentieth International Symposium on Remote Sensing of Environment, Nairobi, Kenya, entitled: *Canopy Reflectance Modeling in Sahelian and Sudanian Woodland and Savannah.*

6. SUMMARY

6.1. Anticipated Problems

We have discussed the strengths of the canopy modeling approach, and explained why we think it will be successful. Now we would like to discuss its weaknesses, the problems we anticipate, and how we will address them.

(1) Characterization of component signatures may be a problem, particularly background signature, which the model is sensative to, and which is highly variable in this region. Image stratification will help reduce this problem — background signature can be assigned empirically within strata. In other words, there may be two strata of the same woodland density class, but with different background signatures.

(2) The highly variable phenology of the herbaceous (understory) and tree layer may make it difficult to apply this model over large areas, or on a repetitive basis as a monitoring technique. Greening up of grasses and leafing out of trees can occur locally (in time or space) in response to rainfall events. This is more of a problem in the Sahelian zone. Also in the Sahelian zone, although the leafing of trees lags behind greening of grasses for most species or vegetation types (trees remain green for at least part of the dry season) there is overlap, and particularly in the inundation zones where tree cover is densest, and signature discrimination between trees and background may be difficult. This can be addressed in the second year when multi-date imagery can be used for signature definition, as well as stratification.

(3) Most of the Sahelian zone has extremely low woody cover. An important question will be what the lower density limits of the model are — when does the tree signal get lost in the noise of background variation? Trees can be identified of high resolution air photos at very low density (2-3%), but can they in satellite imagery, using the model? And, how important is it to recognize densities this low?

(4) Signature and parameter extension — How generalizable are the parameters of the model in this environment? Can the same shape, size distribution and pattern parameters for trees be

extrapolated to other stands in the same strata, and over how great a biogeographic range? At what spatial scale does an atmospheric variation affect the accuracy of the model? If the model parameters are very site-specific, then its inversion is theoretically interesting, but not very practically applicable. This will be addressed in the second year, when the model will be tested in new sites.

6.2. Discussion

By modifying and extending an invertible canopy reflectance model to tropical savanna, we anticipate the following results:

(1) Through exploration of the reflectance model, an improved understanding of the interaction between land surface, radiation, and sensor, particularly the effects of scale-dependent patterns and architecture of the objects in the scene.

(2) Through application of the model using Landsat imagery, an improved ability to extract information on biophysical parameters of the land from remotely sensed data.

(4) Through field measurements required for modeling, cooperation with ongoing intensive field investigations, and by applying remotely sensed data as an additional measurement tool, an improved understanding of the structure, distribution and dynamics of the savanna ecosystem.

This last point has implications at both regional and global scales. An increase in the fundamental knowledge of the factors underlying vegetation distribution will provide basic input for planning at a regional level in an area that is under extreme human population pressure. Also this study will provide information presently lacking on the temporal and spatial dynamics of savanna ecosystems for input into global ecological and climatological models. We anticipate that through functionally relating physiognomic and physiographic pattern on the landscape to image spatial and temporal pattern, a previously underexploited layer of data can be added to the process of information extraction from multiresolution, multitemporal, and multispectral remotely sensed data.

7. REFERENCES

NASA (National Aeronautics and Space Administration), *Land-Related Global Habitability Science Issues*, July, 1983. NASA Technical Memorandum 85841

Ajtay, G. L, P. Ketner, and P. Duvigneaud, "Terrestrial primary production and phytomass," in *The Global Carbon Cycle*, ed. B. Bolin, E.T. Degens, S. Kempe and P. Ketner, pp. 129-181, SCOPE 13, John Wiley and Sons, New York, 1979.

Allen, J. C., "Deforestation, Soil Degradation, and Wood Energy in Developing Countries," PhD dissertation, Department of Geography and Environmental Engineering, The Johns Hopkins University, Baltimore, Maryland, 1983.

Aubréville, A., *Climats, foret et desertification de l'Afrique tropicale*, p. 351, Soc. Ed. Geogr. Marit-et Cd., Paris, 1949.

Bernhardt-Reversat, F., "Observations sur la mineralisation in situ de l'azote du sol en savane sahelienne (Senegal)," *Cah. ORSTOM ser Biol.*, vol. 12, pp. 301-306, 1977.

Bille, J. C., "Mesure de la production primaire appetee des ligneux," in *Browse in Africa*, ed. H. N. Le Houerou, pp. 183-193, ILCA, Addis Ababa, 1980.

Boudet, G., *Rapport sur la situation pastorale dans les pays du Sahel*, p. 45, FAO/EMASAR, IEMVT, Rome, 1975.

Bourlîere, F. and M. Hadley, "Present-day Savannas: An Overview," in *Tropical Savannas*, ed. F. Bourlîere, pp. 1-18, Elsevier Scientific Publishing Company, Amsterdam, 1983.

Breman, H., "La Productivite des Herbes Perennes et des Arbres," in *La Productivite des Paturages Saheliens: Une etude de l'exploitation de cette ressource naturelle*, ed. F. W. T. Penning de Vries and M. A. Djitéye, pp. 284-296, Centre for Agricultural Publishing and Documentation, Wageningen, Holland, 1982.

Breman, H. and C. T. de Witt, "Rangeland productivity and exploitation in the Sahel," *Science*, vol. 221, pp. 1341-1347, 1983.

Card, D. H., "Using known map category marginal frequencies to improve estimates of thematic map accuracy," *Photogrammetric Engineering and Remote Sensing*, vol. 48, pp. 431-439, 1982.

Charney, J. G., P. H. Stone, and W. J. Quirk, *Science*, vol. 191, pp. 100-102, 1975.

Chevallier, A., "Les zones et les provinces botaniques de l'AOF," *C. R. Acad. Sci. CXXX*, vol. 18, pp. 1205-1208, 1900.

Cissé, A. M. and H. Breman, "La Phytoécologie du Sahel et du Terrain d'Etude," in *La Productivite des Paturages Saheliens: Une Etude des Sols, des Végétations et de l'exploitation de cette ressource naturelle*, ed. F. W. T. Penning de Vries and M. A. Djitéye, pp. 71-82, Centre for Agricultural Publishing and Documentation, Wageningen, 1982.

Cissé, M. I., "Effets de divers regimes d'effeuillage sur la production foliare de quelques buissons fourragers de la zone Soudano-Sahelienne," in *Browse in Africa*, ed. H. N. Le Houerou, pp. 209-212, ILCA, Addis Ababa, 1980. a.

Cissé, M. I., "Production fouragere de quelques arbres Saheliens: relations entre biomasse foliar maximale et divers parametres physiques," in *Les fourages ligneux en Afrique*, ed. H. N. Le Houérou, pp. 203-208, International Livestock Center for Africa, Addis Ababa, Ethiopia, 1980. b.

Colwell, J. E., "Landsat feature enhancement or, can we separate vegetation from soil?," in *Proceedings of the 15th International Symposium on Remote Sensing of Environment*, pp. 599-621, Ann Arbor, Michigan, 1981.

Curran, P., "Multispectral remote sensing of vegetation amount," *Progress in Physical Geography*, vol. 4, pp. 315-341, 1980.

Delwaulle, J. C., "Desertification de l'Afrique au sud du Sahara," *Bois et Forêts des Tropiques*, vol. 149, pp. 3-20, 1973.

Dregne, H. E., *Desertification of Arid Lands*, Elsevier, New York, 1983. 242 pp.

Franklin, J., "An empirical study of the spatial pattern of coniferous trees," Masters Thesis, Department of Geography, University of California, p. 99, Santa Barbara, 1983.

Franklin, J. and A. Getis, "A second order analysis of the spatial pattern of Ponderosa pine," *American Association for the Advancement of Science, annual meeting*, Los Angeles, California, 1985.

Franklin, J., T. L. Logan, C. E. Woodcock, and A. H. Strahler, "Coniferous forest classification and inventory using Landsat and digital terrain data," *IEEE Transactions on Geoscience and Remote Sensing*, vol. GE-24, pp. 139-149, 1986.

Franklin, J., J. Michaelsen, and A. H. Strahler, "Spatial analysis of density dependent pattern in coniferous forest stands," *Vegetatio*, vol. 64, pp. 29-36, 1985.

Goel, N. S. and D. E. Strebel, "Inversion of vegetation canopy reflectance models for estimating agronomic variables. I. Problem definition and initial results using the Suits model," *Remote Sensing of Environment*, vol. 13, pp. 487-507, 1983.

Goel, N. S., D. E. Strebel, and R. L. Thompson, "Inversion of vegetation canopy reflectance for estimating agronomic variables. II. Use of angle transforms and error analysis as illustrated by the Suits' model," *Remote Sensing of Environment*, vol. 15, pp. 77-101, 1984.

Goel, N. S., D. E. Strebel, and R. L. Thompson, "Inversion of vegetation canopy reflectance for estimating agronomic variables. II. Use of angle transforms and error analysis as illustrated by the Suits' model," *Remote Sensing of Environment*, vol. 15, pp. 77-101, 1984.

Goel, N. S. and R. L. Thompson, "Inversion of vegetation canopy reflectance for estimating agronomic variables. IV. Total inversion of the SAIL model," *Remote Sensing of Environment*, vol. 15, pp. 237-253, 1984. b.

Graetz, R. D. and M. R. Gentle, "The relationships between reflectance in the Landsat wavebands and the composition of an Australian semi-arid shrub rangeland," *Photogrammetric Engineering and Remote Sensing*, vol. 48, pp. 1721-1730, 1982.

Grieg-Smith, P., *Quantitative Plant Ecology*, Butterworths, London, 1964. 256 pp.

Haralick, R. M. and K. Fu, "Pattern recognition and classification," in *Manual of Remote Sensing, 2nd edition, v. 1*, ed. D. S. Simonett, pp. 793-805, American Society of Photogrammetry, Falls Church, Virginia, 1983.

Hare, F. K., "Climate on the desert fringe," in *Mega-Geomorphology*, ed. R. Gardener and H. Scoging, pp. 134-151, Clarendon Press, Oxford, 1983.

Heimes, F. J. and J. A. Smith, "Spectral Variability in mountain terrain," Final Report, Rocky Mountain Forest and Range Experiment Station U. S. Forest Service Cooperative Agreement 16-625-CA, 1977.

Hiernaux, P., M. I. Cissé, and L. Diarra, "Bilan d'une saison d'es pluies 1984 tres deficitaire dans la Gourma (Sahel Malien). Première campagne de suivi et télédetection expérimentale, Annexe: Fiches descriptives des sites," Programme des Zones Aride et Semi-aride, Document du Programme, CIPEA, Bamako, Mali, 1984.

Hiernaux, P. and C. O. Justice, "Suivi du developpement vegetal au cours de l'ete 1984 dans le Sahel Malien," *International Journal of Remote Sensing*, 1986. In press.

Houghton, R. A., J. E. Hobbie, J. M. Melillo, B. Moore, B. J. Peterson, G. R. Shaver, and G. M. Woodwell, "Changes in the carbon content of the terrestrial biota and soils between 1860 and 1980: A net release of carbon to the atmosphere," *Ecol. Mon.*, vol. 53, pp. 235-262, 1983.

Jackson, R. D., R. J. Reginato, P. J. Pinter Jr., and S. B. Idso, "Plant canopy information extraction from composite scene reflectance of row crops," *Applied Optics*, vol. 18, pp. 3775-3782,

1979.

Jensen, J., "Biophysical remote sensing," *Ann. Assoc. Am. Geog.*, vol. 73, pp. 111-132, 1983.

Justice, C. O., J. R. G. Townshend, B. N .Holben, and C. J .Tucker, "Analysis of the phenology of global vegetation using meteorological satellite data," *International Journal of Remote Sensing*, vol. 6, pp. 1271-1318, 1985.

Lanley, J. P. and J. Clement, "Tropical Forest Resources Assessment Project (in the framework of GEMS - Global Environmental Monitoring System)," *Forest resources of tropical Africa, Part 1- Regional Synthesis*, UN FAO/UNEP (United Nations Food and Agricultural Organization/ United Nations Environmental Programme), Rome, 1982.

Lebrun, J., *Esquisse du Parc National de la Kagera*, Inst. Parcs Natl. Congo Belge, Brussels, 1955. 89 pp.

Le Houerou, H. N., "The rangelands of the Sahel," *Journal of Rangeland Management*, vol. 33, pp. 41-46, 1980.

Li, X., "An invertible coniferous forest canopy reflectance model," Masters Thesis, Department of Geography, University of California, Santa Barbara, 1981. 167 pp.

Li, X., "Geometric-optical modeling of a conifer forest canopy," Ph.D. Dissertation, Department of Geography, University of California, Santa Barbara, CA, 1983.

Li, X. and A. H. Strahler, "Geometric-optical modeling of a conifer forest canopy," *IEEE Transactions on Geoscience and Remote Sensing*, vol. GE-23, pp. 705-721, 1985.

Logan, T. L. and A. H. Strahler, "Optimal Landsat transforms for forest applications," *Proceedings of the 16th International Symposium on Remote Sensing of Environment*, pp. 455-468, Ann Arbor, Michigan, 1982.

Matthews, E., "Global vegetation and land use: New high-resolution data bases for climatic studies," *Journal of Climate and Applied Meteorology*, vol. 22, pp. 474-487, 1983.

Menaut, J. C., "The Vegetation of African Savannas," in *Tropical Savannas*, ed. F. Bourlîere, pp. 109-150, 1983.

Nielsen, M., *Introduction to the flowering plants of West Africa*, University of London Press, London, 1965.

Olsson, K., *Remote sensing of woody vegetation: A quantitative approach in the Sudanese drylands*, Lunds Universitets Naturgeografiska Institution, Lund, 1984. Rapporter och Notiser. Technical report B57.

Olsson, K., "Remote sensing for fuelwood resources and land degradation studies in Kordofan, the Sudan," Ph.D. Dissertation The Royal University of Lund, Sweden, Department of Geography, Lund, 1985. 182 pp.

Otterman, J., "Albedo of a forest modeled as a plane with dense vertical protrusions," *J. Climate and Applied Meteorology*, vol. 22, pp. 297-307, 1984.

Otterman, J., "Bidirectional and hemispherical reflectivities of a bright soil plane and a sparse dark canopy," *International Journal of Remote Sensing*, vol. 6, pp. 897-902, 1985.

Park, M., *Travels in the interior of Africa*, Cassell and Co., Paris, 1893.

Pech, R. P., R. D. Graetz, and A. W. Davis, "Reflectance modelling and the derivation of vegetation indices for an Australian semi-arid shrubland," *Internation Journal of Remote Sensing*, vol. 7, pp. 389-403, 1986.

Penning de Vries, F. W. T. and M. A. Djitéye, *La Productivite des Paturages Saheliens: Une etude de l'exploitation de cette ressource naturelle*, Centre for Agricultural Publishing and Documentation, Wageningen, Holland, 1982.

Petrov, M. P., "Problems preventing the development of deserts and semideserts and their conservation," *Problemy Osvoeniya Pustyn*, vol. 3-4, 1976.

Pielou, E. C., *Mathematical Ecology,* Wiley Interscience, John Wiley and Sons, New York, 1977. 385 pp.

Poupon, H. and J. C. Bille, "Recherches ecologiques sur une savane sahelienne du Ferlo Septentrional, Senegal: Influence de la secheresse de k'annee 1972-1973 sur la strate ligneuse," *La Terre et la Vie,* vol. 28, pp. 49-75, 1974.

Rasool, S. I., "On dynamics of desert and climate," in *The Global Climate,* ed. J. T. Houghton, pp. 107-120, Cambridge University Press, Cambridge, 1983.

Rasool, S. I., M. F. Courel, and R. Kandel, *24th General Assembly COSPAR,* Ottawa, 1982.

Reining, P., *Handbook of Desertification Indices,* Am. Assoc. Adv. Science, Washington, D.C., 1978.

Richardson, A. J., E. C. Weigand, H. Gausman, J. Cuellar, and A. Gerberman, "Plant, soil and shadow reflectance components of row crops," *Photogrammetric Engineering and Remote Sensing,* vol. 41, pp. 1401-1407, 1975.

Rosenfeld, G. H., K. Fitzpatrick-Lins, and H. S. Ling, "Sampling for thematic map accuracy testing," *Photogrammetric Engineering and Remote Sensing,* vol. 48, pp. 131-137, 1982.

Rutherford, M. C., "Woody Plant Biomass Distribution in *Burkea africana* Savannas," in *Ecology of Tropical Savannas,* ed. B. H. Huntley and B. H. Walker, pp. 120-142, 1982.

Schnell, R., *Introduction á la phytogéographie des pays tropicaux: 3. La flore et la Végétation de l'Afrique tropicale,* Gauthiers-Villars, Paris, 1977.

Smith, J. A., "Matter-energy interactions in the optical region," in *Manual of Remote Sensing,* ed. D. S. Simonett, 2nd edition, vol. 1, pp. 61-113, American Society of Photogrammetry, Falls Church, Virginia, 1983.

Sokal, R. R. and F. J. Rohlf, *Biometry,* W. H Freeman & Co., San Francisco, 1969.

Strahler, A. H. and X. Li, "An invertible forest canopy reflectance model," *Proceedings of the Fifteenth International Symposium on Remote Sensing of Environment,* Environmental Research Institute of Michigan, Ann Arbor, 1981.

Strahler, A. H., C. E. Woodcock, T. L. Logan, J. Franklin, H. Bowlin, and J. Levitan, *Automated forest classification and inventory in the Eldorado National Forest,* p. 48, USDA Forest Service, San Francisco, California, 1983.

Strahler, A. H., C. E. Woodcock, and J. Smith, "On the nature of models in remote sensing," *Remote Sensing of Environment,* 1986. accepted for publication.

Suits, G. H., "The calculation of the directional reflectance of a vegetation canopy," *Remote Sensing of Environment,* vol. 2, pp. 117-125, 1972.

Tucker, C. J., J. R. G. Townshend, and T. E Goff, "African land-cover classification using satellite data," *Science,* vol. 277, pp. 369-375, 1985.

Tucker, C. J., C. Vanpraet, E. Boerwinkel, and A Gaston, "Satellite remote sensing of total dry matter production in the Senegalese Sahel," *Remote Sensing of Environment,* vol. 13, pp. 461-474, 1985.

Verhoef, W. and N. J. J. Bunnick, *The spectral directional reflectance of row crops. Part 1: Consequences of non-lambertian behavior for automatic classification. Part 2: Measurements on wheat and simulations by means of a reflectance model for row crops.,* Netherlands Interdepartmental Working Groups on the Application of Remote Sensing, Delft, 1976.

Vinogradov, B. V., "Indicators of desertification and their aerospace monitoring," *Problemy Osvoeniya Pustyn,* vol. 4, pp. 14-23, 1980.

Walker, B. H. and I. Noy-Meir, "Aspects of the Stability and Resilience of Savanna Ecosystems," in *Ecology of Tropical Savannas,* ed. B. J. Huntley and B. H. Walker, pp. 556-590, 1982.

Warren, P. L. and C. Dunford, "Vegetation sampling with large scale aerial photography," *Remote Sensing Newsletter,* vol. 83, pp. 1-6, University of Arizona, 1983.

Woodcock, C. E., "Understanding spatial variability in remotely sensed imagery," Ph.D. dissertation, Department of Geography, University of California, Santa Barbara, 1985. 136 pp.

Woodcock, C. E. and A. H. Strahler, "Characterizing spatial patterns in remotely sensed data," in *Proceedings of the 17th International Symposium on Remote Sensing of Environment*, Ann Arbor, Michigan, 1983.

Woodwell, G. M., *The role of terrestrial vegetation in the global carbon cycle*, p. 247, Wiley, New York, 1984.

Zhan, C., "Grey level dependent texture measures: sensitivity and stability problems and applications in remote sensing," Ph.D. Dissertation, Department of Geography, University of California, Santa Barbara, 1986. 100 pp.

TABLE 1									
Site	Species	n	Stem Size		Height (H)		Crown Radius (R)		Source
			μ	σ	μ	σ	μ	σ	
(Niono)	*A. nilotica*	30	8.9[1]	(4.3)	4.9	(1.8)	1.9[3]	(1.6)	II.
15	*A. nilotica*	71	10.4[1]	(5.7)	5.2	(1.4)	3.0[3]	(2.4)	I.
15	*A. nilotica*	75	10.4[1]	(5.7)	5.3	(1.4)	3.5[3]	(3.4)	I.
(Niono)	*A. seyal*	45	14.5[1]	(8.1)	4.6	(2.0)			II.
20	*A. seyal*	114	8.5[1]	(1.9)	5.2	(0.9)	2.8[3]	(2.0)	I.
21	*A. seyal*	125	4.9[1]	(2.8)			2.1[3]	(1.8)	III.
Niono	*B. aegyptica*	20	8.5[a]	(4.8)	2.7	(1.0)	1.0[3]	(1.2)	I.
3, 4	*A. albida*	62	21.3[2]	(7.3)	12.2	(2.8)	4.8[4]	(1.7)	IV.
1, 2	*V. paradoxa*	65	14.2[2]	(5.8)	7.7	(2.2)	3.7[4]	(1.1)	IV.

Notes:

Stem Size: 1 — basal circumference
2 — diameter at breast height
a — from a different population

Crown Radius: 3 — from estimate of crown surface area
4 — crown diameter measured

Source: I. Hiernaux *et al.* 1984
II. Cissé 1980b
III. Hiernaux 1985, unpublished data
IV. this study

TABLE 2							
Site	Species	n	h	h/R	R^2	σ_{R^2}	$CR\,2$
Niono	*A. nilotica*	30	3.0	1.58	3.8	2.6	0.47
15	*A. nilotica*	71	2.2	0.73	11.9	15.0	1.59
15	*A. nilotica*	75	1.8	0.50	11.9	15.0	1.59
20	*A. seyal*	114	2.4	0.86	7.6	3.8	0.25
21	*A. seyal*	125			4.5	3.3	0.53
Niono	*B. aegyptica*	20	1.7[1]	1.70	1.1	1.4	1.62
3, 4	*A. albida*	62	7.4[2]	1.54	24.8	17.3	0.49
1, 2	*V. paradoxa*	65	4.0[3]	1.10	15.2	9.5	0.39

Notes:

h (height to bottom of canopy) calculated for idealized semisphere shape $(H - R)$

R^2 is the average squared crown radius

$CR\,2$ is the coefficient of variation of $R^2 = V(R^2)/(R^2)^2$.

1 — height to lowest branched measured, = 0.5 m

2 — height to widest part of crown measured, = 8.7 (1.9) m.

3 — height to widest part of crown measured, = 5.1 (1.4) m.

TABLE 3		
	Gourma	Segou
	$\theta = 38.7$	$\theta = 50.8$
h/R	Γ	Γ
0.50	4.37	5.26
0.55	4.45	5.37
0.60	4.53	5.49
0.65	4.61	5.60
0.70	4.69	5.71
0.75	4.76	5.82
0.80	4.84	5.93
0.85	4.91	6.04
0.90	4.99	6.14
0.95	5.06	6.24
1.00	5.14	6.34
1.05	5.21	6.44
1.10	5.28	6.53
1.15	5.35	6.62
1.20	5.42	6.70
1.25	5.49	6.78
1.30	5.56	6.86
1.35	5.63	6.93
1.40	5.70	7.00
1.45	5.76	7.06
1.50	5.83	7.11
1.55	5.89	7.15
1.60	5.95	7.18
1.65	6.01	7.19
1.70	6.07	7.19
1.75	6.13	7.19

TABLE 4
Relationships Among Tree Measurements

Site	Species	n	Regression Equation	R^2
Predict Crown Size (R or S or CW) from Stem Size (DBH or C)				
**	*A. nilotica*	30	$\log S = 1.13 \log C - 1.34$	.88
15	*A. nilotica*	75	$\log S = 1.12 \log C - 0.05$	.59
20	*A. seyal*	114	$\log S = 0.81 \log C + 0.15$	.54
21	*A. seyal*	125	$\log S = 1.24 \log C - 0.09$	.73
3&4	*A. albida*	62	$CW = 0.35\ DBH + 2.20$	.59
1&2	*V. paradoxa*	65	$CW = 0.4\ DBH + 1.33$	.58
Predict Crown Size (R or S or CW) from Height (H)				
**	*A. nilotica*	30	$\log H = 0.49 \log S + 0.41$	.65
15	*A. nilotica*	75	$\log H = 0.23 \log S + 0.88$	.43
20	*A. seyal*	114	$\log S = 2.07 \log S - 0.35$	.47
**	*B. aegyptica*	20	$S = 3.9\ H - 7.15$	.80
3&4	*A. albida*	62	$H = 0.63\ CW + 6.16$	.55
1&2	*V. paradoxa*	65	$H = 0.53\ CW + 4.0$	.37
Predict Height (H) from Stem Size (DBH or C)				
**	*A. nilotica*	30	$\log H = 0.64 \log C - 0.52$	.77
15	*A. nilotica*	75	$\log H = 0.34 \log C + 0.51$	.43
20	*A. seyal*	114	$\log H = 0.7 \log C - 1.13$	.96
21	*A. seyal*	125	$\log H = 0.24 \log C + 0.89$	.42
**	*B. aegyptica*	20	$\log H = 0.46 \log C - 0.49$	.71
3&4	*A. albida*	62	$H = 0.33\ DBH + 5.5$	.51
1&2	*V. paradoxa*	65	$H = 0.31\ DBH + 3.71$	.70

** data from Cissé 1980. (Data for sites 15 and 20 from Hiernaux et al. 1984.)

TABLE 5
Quadrat Analysis: Fit to Poisson Distribution

Quadrat Size	*n* quadrats	*n* points	mean	χ^2	df
Gourma Site 15 (*A. nilotica*)					
10	784	587	0.7	4.7	3
20	196	587	3.0	4.7	9
25	121	567	4.7	8.0	12
30	81	547	6.8	34.1*	13
35	64	587	9.2	9.1	18
40	49	587	12.0	20.9	24
50	25	466	18.6	10	27
Gourma Site 20 (*A. seyal*)					
20	182	838	4.6	10.0	10
25	121	877	7.2	24.8	18
30	81	850	10.5	25.9	19
35	56	780	13.9	15	28
40	42	757	18.0	51*	30
Segou Site 2 (subplot 1) (*V. paradoxa*)					
10	625	223	0.36	3.1	0
20	144	212	1.47	0.3	4
30	64	213	3.3	3.9	7
40	36	213	5.9	5.8	14
50	25	223	8.9	6.4	17
60	16	213	13.1	11.3	26

* significantly different at .05 level

TABLE 6
Actual Tree Size and Density for Test Sites

Site	Percent Cover	Area (ha)	Density (trees/ha)	R^2(*)
Gourma 15: field	31.0	(1 km)		
photo	22.6	9.80		
photo	26.5	7.84	75.1	11.2
Gourma 20: field	59.4	(1 km)		
photo	38.8	9.80		
photo	35.0	7.84	114.2	9.75
Segou 1: field	13.0	4.52[1]	27.6	16.26
Segou 2: field	18.9	3.48[1]	46.4	12.84
photo	26.8	25.00	41.4	20.63
Segou 3: field	21.2	3.14[1]	39.8	16.95
Segou 4: field	14.5	4.52[1]	15.2	30.23

Notes:
* — Calculated from cover area divided by number of trees (see Table 2 for measured R^2)
1 — total area for four subplots

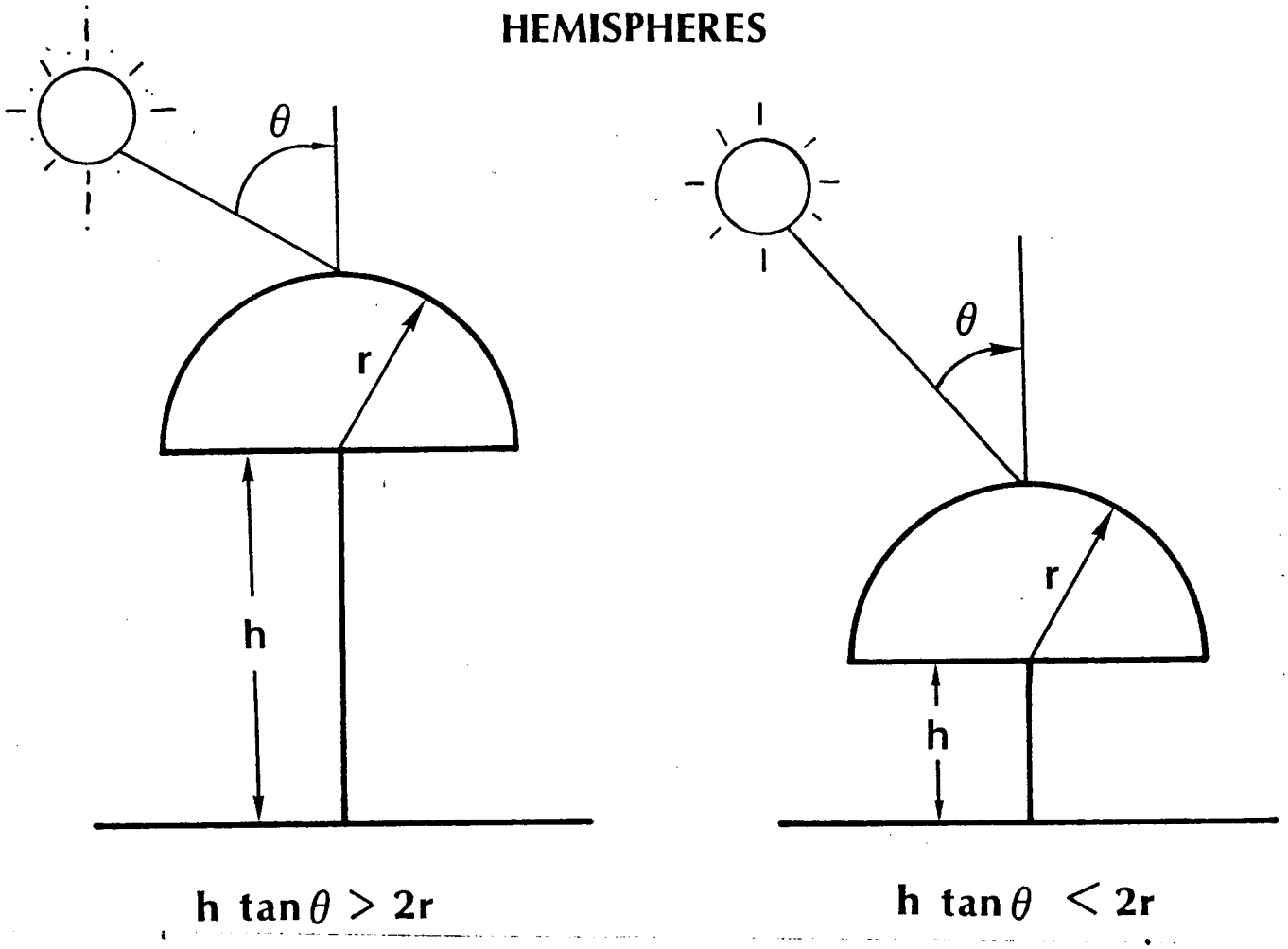

Figure 1. Geometric models for savanna tree shapes; 1) semisphere, 2) inverted cone, and 3) disk on a stick.

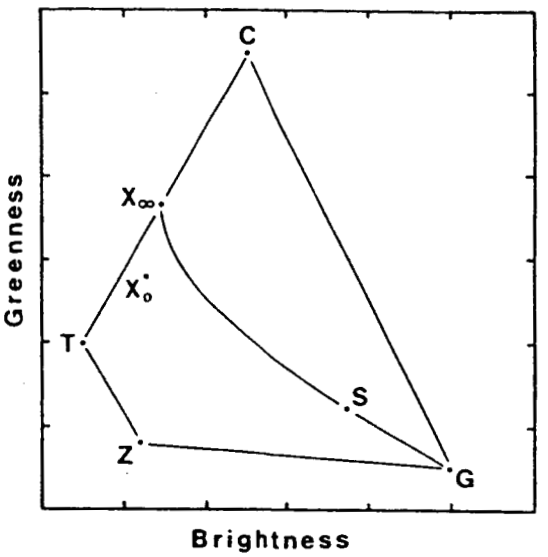

Fig. 2. Idealized plot of brightness–greenness spectral space with component signatures and diagrammatic coverage trajectory.

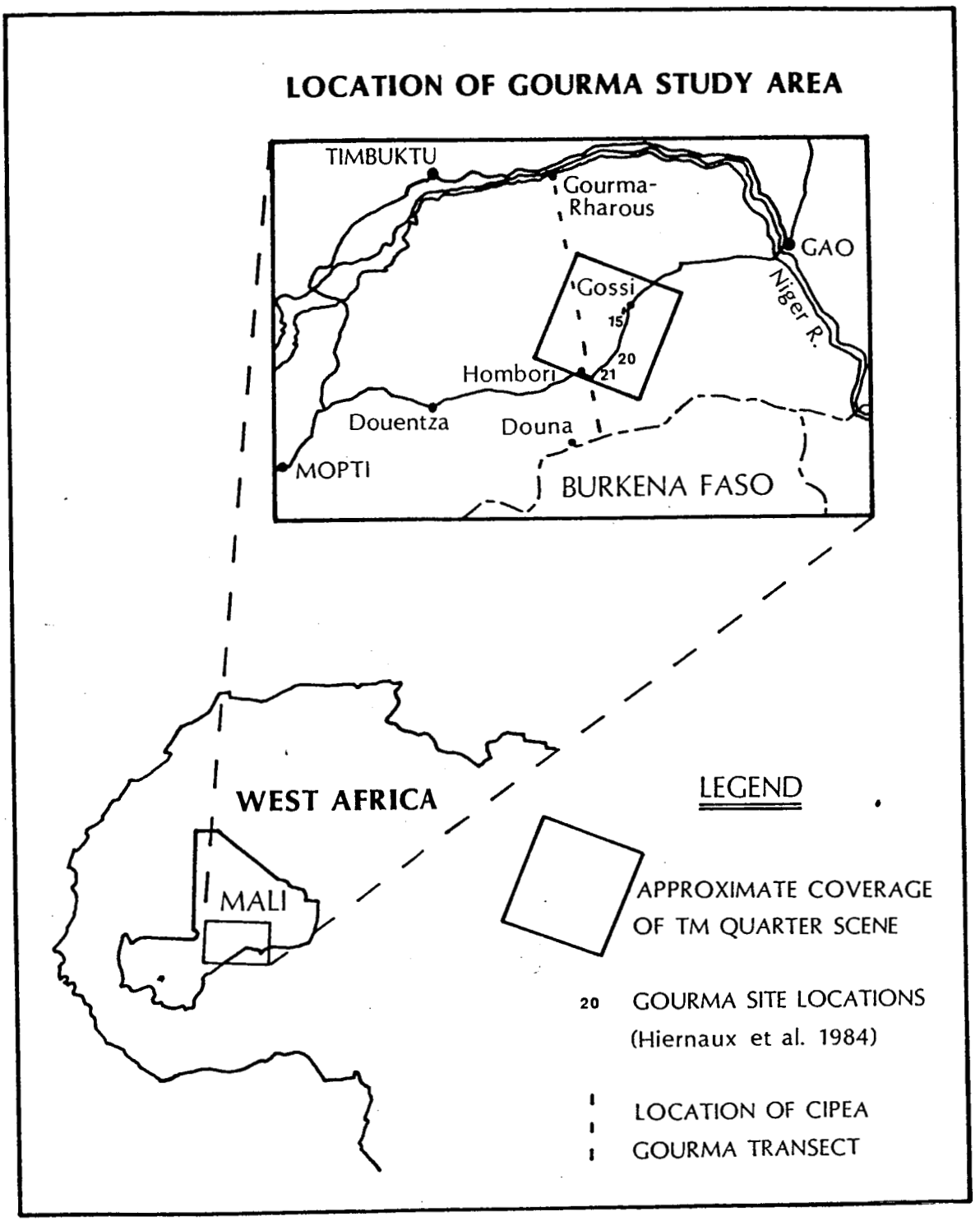

Figure 3. Location of Gourma Study Area.

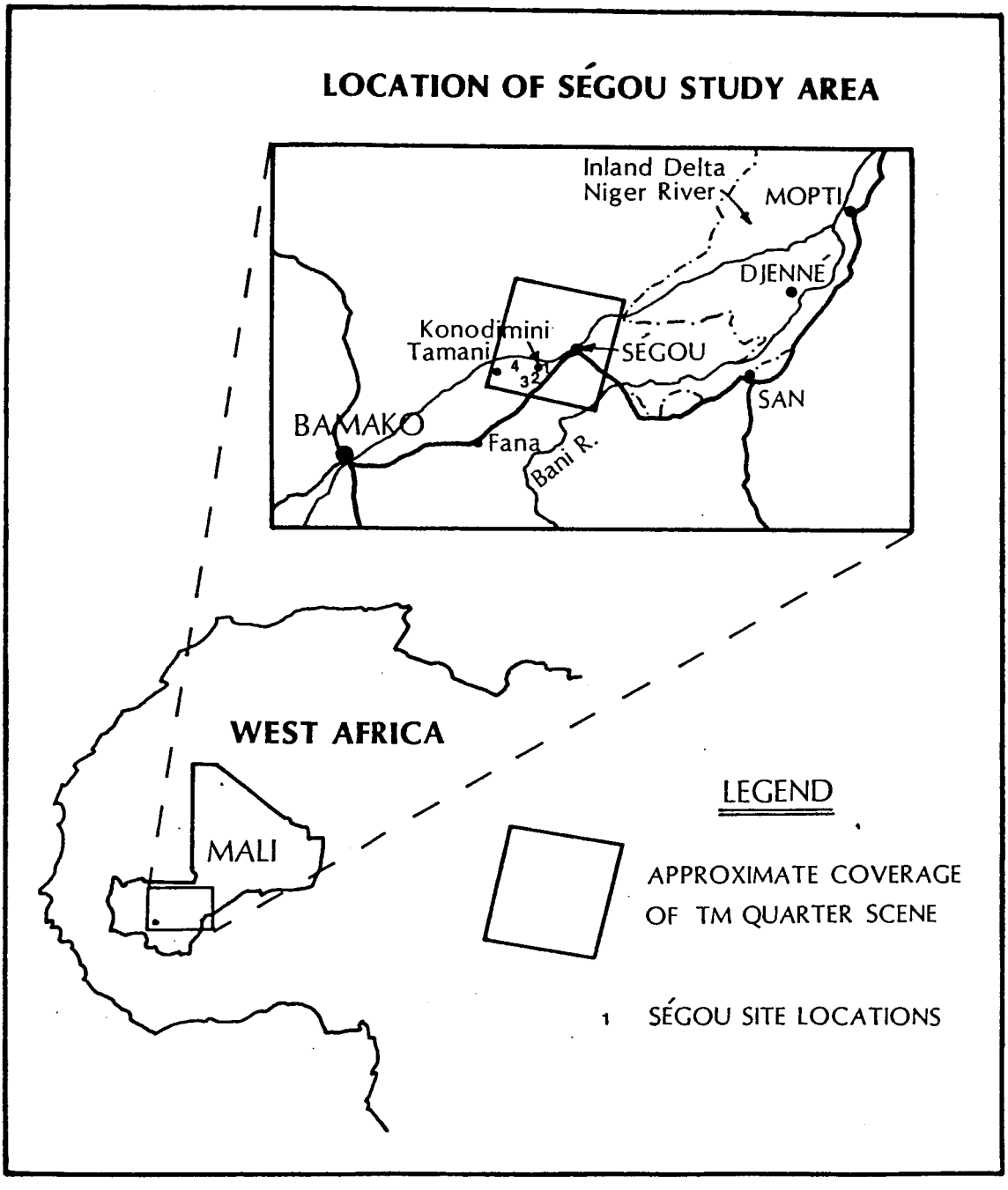

Figure 4. Location of Ségou Study Area.

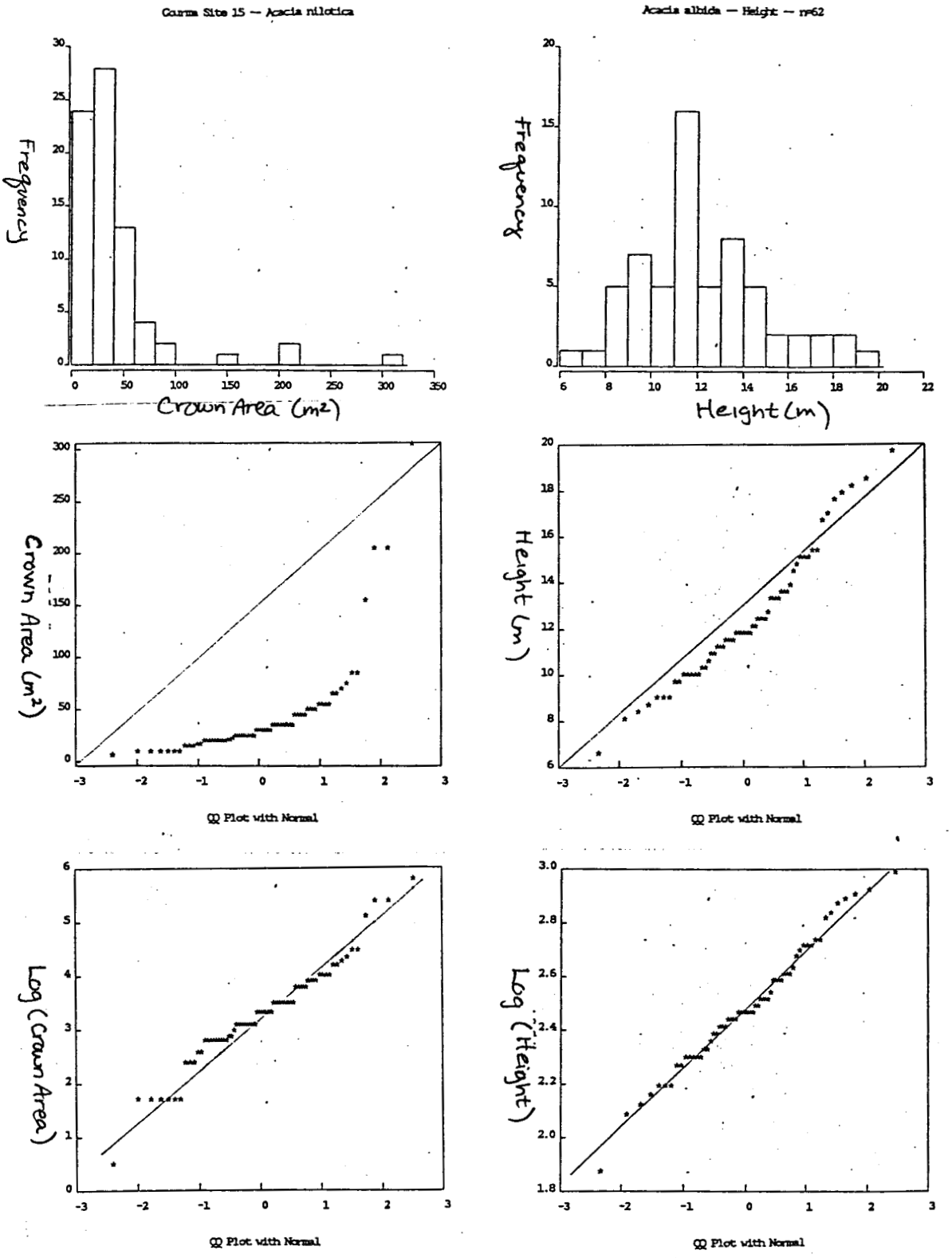

Figure 5. Histograms of size distributions for *Acacia nilotica* and *Acacia albida*. The quantile-quantile (Q-Q) plots represent the data plotted against corresponding quantiles of the normal distribution (units are standard deviations). If the points fall in a straight line, they are normally distributed.

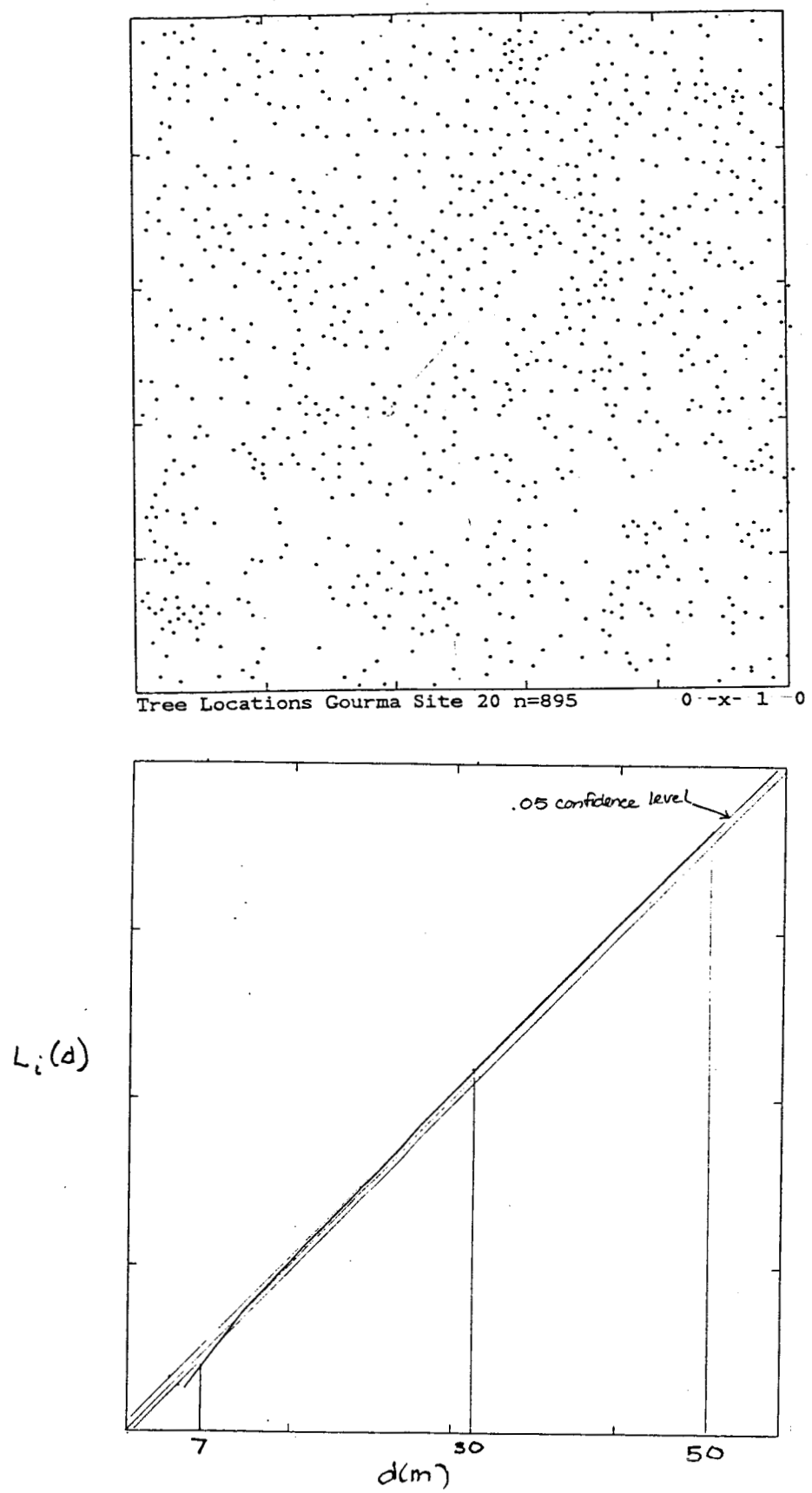

Figure 6. a) Point locations of trees, Gourma Site 20. b) Cumulative frequency of observed interpoint distances ($L_i[d]$). The diagonal is the expected frequency for a Poisson distribution, and the lines surrounding it are the .05 significance level.

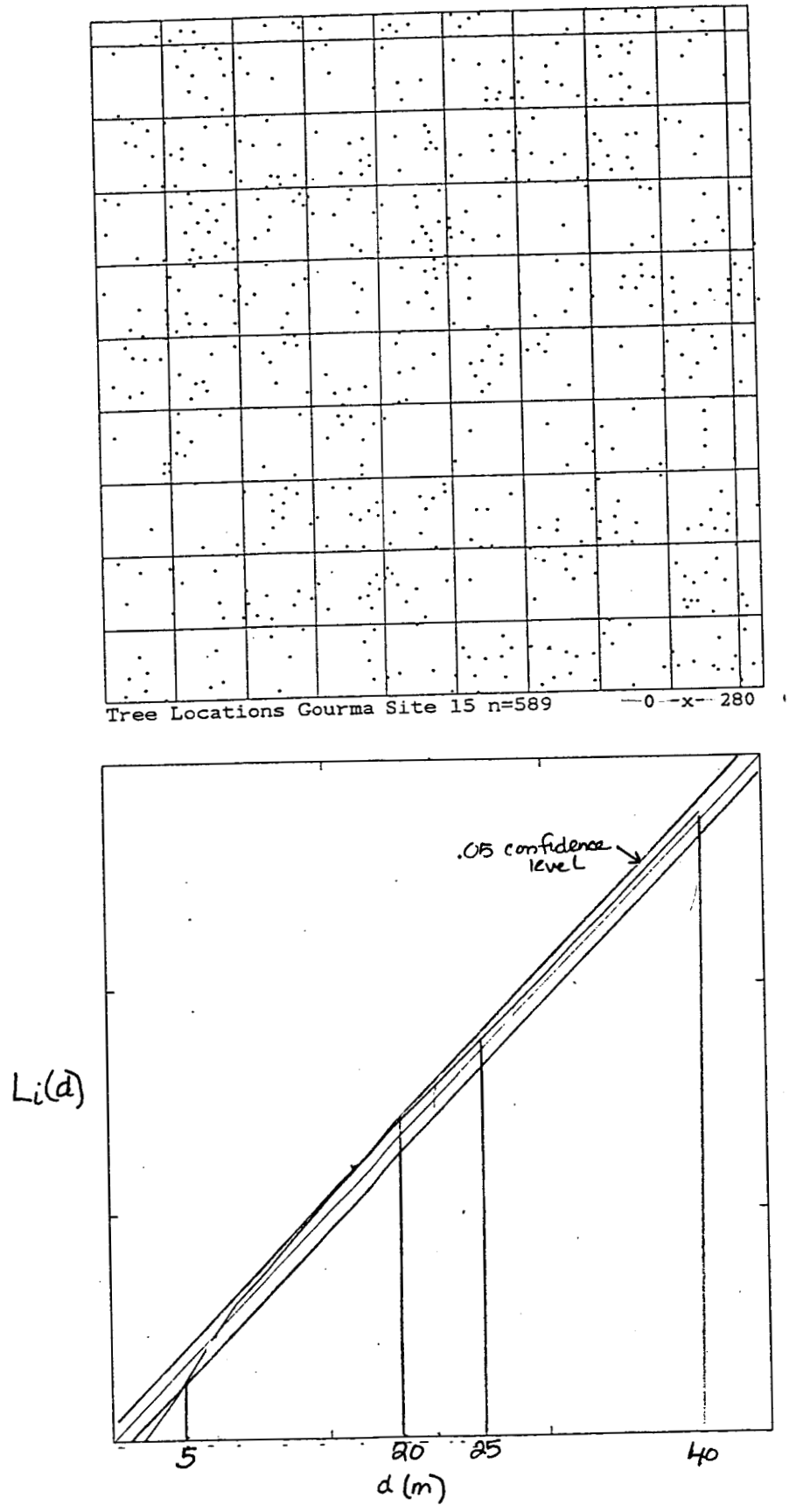

Figure 7. a) Point locations of trees, Gourma Site 15 with grid of 30 m quadrats overlain. b) Cumulative frequency of observed interpoint distances ($L_i[d]$). The diagonal is the expected frequency for a Poisson distribution, and the lines surrounding it are the .05 significance level.

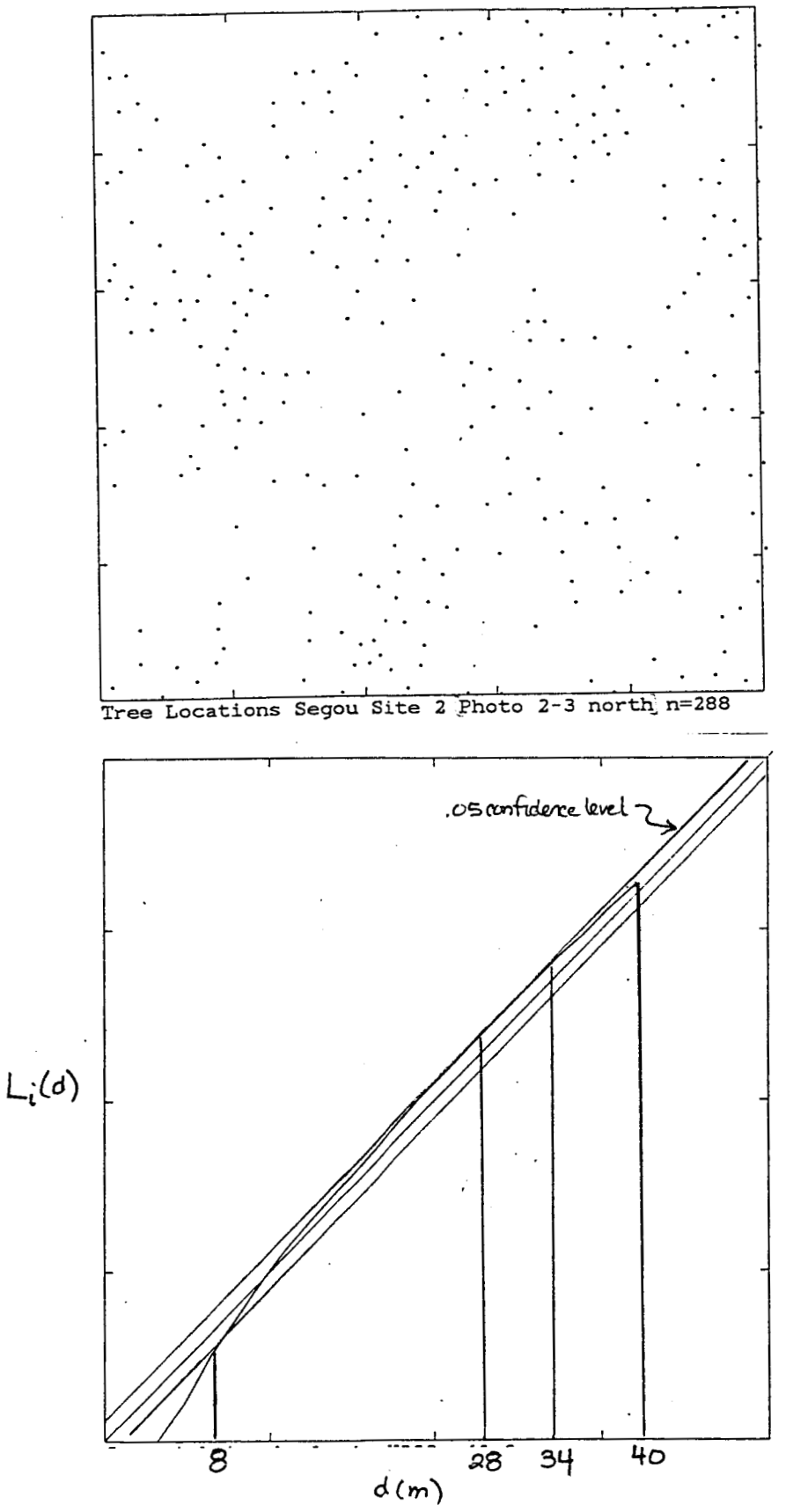

Figure 8. a) Point locations of trees, Ségou Site 2 (subplot 2). b) Cumulative frequency of observed interpoint distances ($L_i[d]$). The diagonal is the expected frequency for a Poisson distribution, and the lines surrounding it are the .05 significance level.

APPENDIX A

CANOPY REFLECTANCE MODELING IN SAHELIAN AND SUDANIAN WOODLAND AND SAVANNAH

Janet Franklin

Department of Geography
University of California
Santa Barbara, CA 93106

Li Xiaowen
Alan H. Strahler

Department of Geology and Geography
Hunter College of the City University of New York
695 Park Ave, New York, New York 10021

(Presented at the Twentieth International Symposium on Remote Sensing of Environment, Nairobi, Kenya, 4-10 December 1986.)

CANOPY REFLECTANCE MODELING IN SAHELIAN AND SUDANIAN WOODLAND AND SAVANNAH

Janet Franklin

Department of Geography
University of California
Santa Barbara, CA 93106

Li Xiaowen
Alan H. Strahler

Department of Geology and Geography
Hunter College of the City University of New York
695 Park Ave, New York, New York 10021

ABSTRACT

A geometric-optical canopy reflectance model, driven by Landsat Thematic Mapper (TM) data, provided direct estimates of tree cover within twenty percent of actual values for several sparse woodland stands in West Africa. This model exploits tree geometry in an inversion technique to predict average tree size and density from reflectance data using a few simple parameters measured in the field (spatial pattern, shape, and size distribution of trees). Trees are treated as simply shaped objects, and multi-spectral reflectance of a pixel is a function of the proportion of tree crown, shadow, and understory in the pixel. These proportions are a direct function of the number and size of trees, and given the variance in reflectance within a homogeneous area of woodland, the model can be inverted to give estimates of average tree size and density. The model was tested in two sites in the Sahelian zone and five sites in the Sudanian zone, Mali. Tree density was consistently overestimated, and tree size underestimated, but correlation between observed and predicted values was very good ($r^2 > .85$). After improving our method for selecting component spectral signatures (for tree and background) results improved dramatically for stand estimates of tree size and density.

1. INTRODUCTION

A family of mathematical models of the reflectance of a plant canopy composed of discontinuous woody cover allows the direct estimation of plant size and density from remotely sensed reflectance data (Li and Strahler 1985). The models are geometric in character, treating trees (plants) as solid objects on a contrasting background, and estimating the proportion of each pixel in tree canopy, shadow, and background. In the simplest model, tree density is assumed to be low, and trees and shadows do not overlap enought to change the proportion of shadow in a pixel. Using this simple model, Li and Strahler (1985; Strahler and Li 1981) predicted tree size and density within ten percent of actual values for sparse pine forest in northern California from Landsat MSS data.

We have extended this model and tested it using Landsat Thematic Mapper (TM) data in a new environment where the basic assumptions of the model hold, but the parameters must be modified. The model was tested in sparse woodland and wooded grassland in the Sahelian and Sudanian bioclimatic zones in West Africa. Dry woodlands and wooded grasslands are important ecologically and economically in Africa, and cover forty percent of the continent by some estimates. The depletion of woody cover due to changes in land use practices, coupled with increasing population and

*Presented at the Twentieth International Symposium on Remote Sensing of Environment, Nairobi, Kenya, 4-10 December 1986

drought, is a severe problem for people living in these areas where trees are used for fuel and fodder.

Our method can be used as part of a multi-stage inventory to directly estimate the size and density of woody plants over large areas. Because size and spacing are often related to leaf and woody biomass, this technique could also provide woodland biomass estimates over large areas.

Further, an important application of global remote sensing is the estimation of ecosystem productivity using spectral greenness measures from the AVHRR sensor (Justice et al. 1985, Tucker et al. 1985a, Tucker et al. 1985b). One problem with this approach is that the relationship between the spectral index and green biomass is affected by woody cover (and other factors such as soil background and atmosphere; Hiernaux and Justice 1986, Holben and Fraser 1984). Our model could help improve these methods by providing tree density estimates within vegetation strata, for adjusting the greenness index/biomass relationship.

2. BACKGROUND

Plant canopy modeling provides a way of understanding the reflectance of a vegetated surface by building a functional model of reflectance based on the biophysical, optical, and spatial properties of the scene elements (plants or plant parts). If a reflectance model can be *inverted* the biophysical properties of the plant stand can be inferred from spectral reflectance measurements. The simple Li-Strahler model uses covariance statistics from estimated mixtures of scene components across pixels for inversion, to predict average tree size and density in a stand. This model is discussed in great detail in Li and Strahler (1985) and Li (1983) and will only be described briefly here. The assumptions of the model are as follows:

- a tree crown is a simple geometric form, in this case a hemisphere on a stick (Fig. 1).
- tree counts vary from pixel to pixel as a Poisson function with a fixed density (e. g. — the spatial pattern is random at the scale of sensor resolution)
- the size distribution function of trees is known, so that C_{R^2}, the coefficient of variation of squared crown radius, can be determined for the stand.
- the tree crown and its associated shadow have a spectral signature which is distinct from that of the understory (background).

The reflectance of a pixel is modeled as a linear combination of the signatures of scene components (tree crown, background, shadowed tree and background) weighted by their relative areas. Pixels from an area of homogeneous tree cover can be taken as replicate measures of reflectance. Interpixel variance comes from variance in the number of trees among pixels and variation in the size of trees within and between pixels (if chance overlapping of trees and shadows is ignored).

From the reflectance values the parameter m ($= NR^2$) can be calculated, where N is the average tree density, and R^2 the average squared crown radius. Note that $m\,\pi$ is equal to the proportion of woody cover in the stand. If N and R^2 are uncorrelated (a reasonable assumption is a sparse stand) then the expression for mean and variance of two independent products will apply, and mean size and density can be separated using the mean and variance of stand reflectance.

The model also includes a geometric factor, Γ, which is defined such that $m\,\Gamma$ is the proportion of a pixel covered by tree crown and shadow. Γ can be calculated from the tree-shape geometry and the sun angle. The reflectance signatures of the model are:

- G Reflectance vector for a unit area of illuminated background (constant).
- C Reflectance of a unit area of illuminated crown (constant).
- Z Reflectance of a unit area of shadowed background (constant).
- T Reflectance of a unit area of shadowed crown (constant).
- S Reflectance of a pixel. Variable; depends on number and size of trees in pixel.
- $V(S)$ Variance in reflectance of all pixels in a stand.

The signature of pixel i in band j is then modeled as

$$S_{ij} = G_j \cdot K_g + (1-K_g)\cdot(C_j \cdot K_c + Z_j \cdot K_z + T_j \cdot K_t)\,. \qquad (1)$$

where

K_g Proportion of pixel not covered by crown or shadow.

K_c Proportion of area covered by crown and shadow that is in illuminated crown.

K_t Proportion of covered area in shadowed crown.

K_z Proportion of covered area in shadowed background.

Because K_c, K_z, and K_t sum to one (by definition), the expression $(C_j \cdot K_c + Z_j \cdot K_z + T_j \cdot K_t)$ represents a point in multispectral space lying within a triangle with vertices at C, Z, and T (see Figure 1). This point is X_0; the average reflectance of a tree and its associated shadow. When m varies, S will vary along a straight line connecting points G and X_0.

The area of a pixel which is not background $(1 - K_g)$ was previously defined as $m\Gamma$. So, $K_g = 1 - m\Gamma$. Therefore, dropping the subscripts, (1) can be written

$$S = G(1 - m\Gamma) + X_0 m\Gamma$$

and rearranging, we have

$$m = \frac{G - S}{\Gamma(G - X_0)} . \tag{2}$$

From (2) we can derive the variance of m:

$$V(m) = \frac{V(S)}{\Gamma[(G - X_0)]^2} . \tag{3}$$

In the multiband case, m should be the same if determined from any band. However, variance in the signatures and stand parameters will cause m to vary, and thus m can be taken as a weighted average. Because $(G - X_0)$ is in the denominator, sensitivity to variance and noise in S, G and X_0 will be reduced when spectral contrast between trees and background is high.

If size and density are independent, then the mean and variance of m are the mean and variance of independent products, and the following expressions apply:

$$M = E(nR^2) = E(n) \cdot E(R^2) = N\mathbf{R}^2 , \tag{4}$$

and

$$V(m) = V(nR^2) = (\mathbf{R}^2)^2 V(n) + N^2 V(R^2) + V(n)V(R^2) . \tag{5}$$

Because n is a Poisson function,

$$V(n) = N . \tag{6}$$

Further,

$$V(R^2) = V(r^2)/n \approx V(r^2)/N = C_{R^2}(E(r^2))^2/N \tag{7}$$

because $C_{R^2} = V(r^2)/(E(r^2))^2$. Substituting (6) and (7) into (5),

$$V(m) \approx (N + C_{R^2} N + C_{R^2})(\mathbf{R}^2)^2 = (M + C_{R^2} M + C_{R^2} \mathbf{R}^2)\mathbf{R}^2 . \tag{8}$$

Solving for $\mathbf{R}^2$, we obtain:

$$\mathbf{R}^2 = \frac{[(1 + C_{R^2})^2 M^2 + 4V(m)C_{R^2}]^{1/2} - (1 + C_{R^2})M}{2C_{R^2}} . \tag{9}$$

Applying the approximation $\sqrt{1 + x} \approx 1 + x/2$, we obtain

$$\mathbf{R}^2 = \frac{V(m)}{(1 + C_{R^2})M} . \tag{10}$$

Finally, substituting (2) and (3), the expressions for mean and variance of m, into (10), R^2 can be found from the reflectance values of a pixel in a stand, and the N can be found using (4).

3. STUDY SITES IN MALI

Sahelian test sites in the Gourma region of Mali were chosen from among those being monitored by ILCA/Mali (The International Livestock Centre for Africa) in collaboration with the GIMMS Project (Global Inventory, Monitoring and Modeling System; National Aeronautics and Space Administration, Goddard Space Flight Center). Two sites were used for the initial test of the model, ILCA Sites 15 and 20. Site 15 is located in an *Acacia nilotica* woodland (approximately 31 percent cover), on an alluvial plain of poorly drained vertisols. Site 20 is located in an *Acacia seyal* woodland (approximately 58 percent cover), also on an alluvial plain of vertisols that is inundated during the rainy season, but more freely drained that Site 15 (Hiernaux *et al.* 1984).

The Sudanian test sites are located in the Region of Ségou. The crop/woodland type of vegetation is formed when crops are grown under a woodland of useful trees which are preserved when land is cleared. Sites 1 and 2 are dominated by *Vitellaria paradoxa* (called shea, karité, or shi), and Sites 3, 4N and 4S are dominated by *Acacia albida* (balanzan). All sites are located in the house fields (cultivated areas near the village where shrubs and weeds are cleared regularly) and cover range from 13 to 25 percent.

4. METHODS

A hemispherical shape was initially chosen to test the model in savanna, based on field reconnaissance. Tree height (H) and crown diameter ($= 2r$) were measured for thirty to one hundred trees in each site, and average h (see Fig. 1) was calculated from $H - R$ for the stand. The ratio h/R was used to calculate Γ from the geometry of the hemisphere. Size distribution was examined by inspecting histograms of tree size (expressed both as crown size and height) for all sites. The model parameter C_{R^2} was calculated from sample data for the sites. Spatial pattern was established by mapping point patterns of 200-900 trees from low-altitude aerial photographs in sample quadrats within the test sites, and analyzing using quadrat analysis (Li and Strahler 1981, Franklin et al. 1985), and second-order analysis of inter-tree distances (Franklin and Getis 1985).

Landsat Thematic Mapper (TM) data were used to test this model. Early dry season imagery was chosen to enhance the contrast between trees (still green for most species) and understory (a dry herbaceous layer, or bare soil). The TM scene for the Gourma sites was acquired 9 September 1984 at the end of a very bad growing season in the Sahel. The scene for the Ségou sites dates from 17 November 1984, after the harvest, so the fields beneath the canopy have been cleared. The mean and variance of reflectance (S and $V(S)$) were computed for each of the test sites. Signatures for background and canopy (G and X_0) were computed from small training areas in the image, using aerial photographs as a guide. Areas of no tree cover in or near sites were used to estimate G, and pixels with high tree cover were used to estimate X_0.

The model was tested by inputting the stand parameters (Γ and C_{R^2}) and the spectral parameters (G, X_0, S and $V(S)$), predicting R^2 and N for each site, and comparing to actual R^2 and N from field measurements. Observed and predicted values were compared by simple regression. The model was tested using TM Bands 3 (.63-.69 μm) and 7 (2.08-2.35 μm). Band 3 was chosen because in our experience red reflectance is strongly related to tree cover (Logan and Strahler 1982, Franklin 1986), and Band 7 had the highest variance in the sites, and has also been shown to be related to tree cover (Horler and Ahern 1986).

5. RESULTS

Table I shows the stand parameters h/R, R, C_{R^2} and Γ for all sites. Values for H/R range from 1 to 1.6 for Ségou sites (taller trees, narrower crowns) and 0.5 to 0.6 for Gourma sites (shorter trees, wider crowns). C_{R^2} values range from 0.21 to 0.69.

Tree size distributions for all sample populations were slightly to extremely right-skewed, and a log-transform produced a normal-looking distribution (Fig. 3). Thus, if field measurements were not available, the assumption of a lognormal size distribution is supported for these sites, and the formula for C_{R^2} for a lognormal distribution could be used. However, for these sites C_{R^2} was calculated directly from sample data.

Table I. Stand Parameters

Site	Species	n	h/R	R	C_{R^2}	Γ
15	*A. nilotica(*)*	56	.50	3.63	.6850	4.37
20	*A. seyal(*)*	87	.62	3.23	.4401	4.55
1	*V. paradoxa*	33	1.22	3.62	.6166	6.73
2	*V. paradoxa*	32	1.06	3.88	.2560	6.44
3	*A. albida*	32	1.50	4.44	.2672	7.11
4N	*A. albida*	14	1.17	6.57	.2125	6.63
4S	*A. albida*	16	1.64	4.66	.3816	7.19

Fig. 4 shows the point locations and results of second order analysis for one of the sites. In all sites there is generally an inhibition distance of five to ten meters, below which the probability of finding two trees is very low, but at relevant sensor resolution (20 to 50 m) a Poisson model is adequate. This is supported by the quadrat analysis. At larger distances (50 to 100 m) a Poisson model still fits in many of the sites, including the sparser stands (Site 2) at densities where the Poisson model broke down in our earlier studies (Franklin et al. 1985).

The results of the model test are shown in Table II which includes the model parameters and observed and predicted values values of R^2 and N. The model consistently overestimates density and underestimates crown size, but predicted cover values are very close to actual cover based on field measurements, and there is good correlation between observed and predicted values of N and R^2 (Table IV). Table III shows the rank order of observed and predicted R^2, N and Cover for TM Bands 3 and 7. Rank order is preserved in most cases. The model easily separates big crown, low density stands from large crown, high density stands.

Table II. Results Canopy Model Inversion TM Band 3 (.63–.69μm)

Site	G_{ob}	G_{pr}	X_{0ob}	X_{0pr}	S	$V(S)$	Area(ha)	$R^2_{ob}(m^2)$	R^2_{pr}	No (/piz)	N_{pr}	C_{ob}	C_{pr}	%
15	149.9	137.6	108.5	108.2	124.7	43.4	71.6	14.04	5.04	6.42	24.66	.31	.44	70
20	151.9	141.0	102.2	114.8	119.1	44.4	72.0	10.62	3.78	15.57	34.92	.58	.46	79
1	103.1	102.4	68.7	72.1	90.7	59.4	51.8	13.86	11.43	3.73	4.22	.18	.17	94
2	98.2	95.4	68.7	58.1	84.8	56.9	92.5	16.02	16.02	2.48	3.97	.14	.22	64
3	98.2	96.9	79.0	77.0	86.7	37.1	86.2	18.18	16.74	3.58	4.52	.23	.26	88
4N	110.5	106.4	83.0	86.8	95.9	83.3	25.2	45.63	23.13	1.59	3.28	.25	.26	96
4S	108.6	104.0	83.0	86.4	98.7	24.6	18.1	24.21	8.82	1.55	5.50	.13	.17	76
Using X_0 and G from 4N,								predict R^2 and N						
4S	106.4		86.8		98.7	24.6		24.21	14.76	1.55	3.33	.17	.17	100

Table III. Rank Order of Predicted and Observed Size, Density and Cover

Band 3		Band 7		Band 3		Band 7		Band 3		Band 7	
R^2				N				*Cover*			
Pred	Obs	Pred	Obs	Pred	Obs	Pred	Obs	Pred	Obs	Pred	Obs
20	20	20	20	4N	4S	2	4S	4S	4S	4S	4S
15	1	15	1	2	4N	4S	4N	1	2	2	2
4S	15	1	15	1	2	4N	2	2	1	1	1
1	2	4S	2	3	3	3	3	3	3	3	3
2	3	3	3	4S	1	1	1	4N	4N	4N	4N
3	4S	4N	4S	15	15	15	15	15	15	15	15
4N	4N	2	4N	20	20	20	20	20	20	20	20

We noted that it is difficult to accurately characterize component signatures using training data. Using our training technique, the observed G was too bright, and observed X_0 too dark in most cases. Overestimating G caused the individual predictions of N to be too high, and R^2 too low. Therefore, our next approach was to predict the component signatures (G and X_0) using the model, based on observed N and R^2 for the sites. Table II shows predicted values of G and X_0. In all cases there is a good correlation between observed and predicted spectral variables (G and X_0); see Table IV. To see if signature extension is possible, predicted values of G and X_0 from Site 4N were used to predict N and R^2 in Site 4S (same type of woodland, different size and density). The bottom entry in Table II show that the predicted values match observed more closely when component signatures are predicted from the model, and then extended in this way.

Table IV. Regression Equations and r^2 for Observed and Predicted Values

Variable	Band	Regression Equation	r^2
R^2	3	$Obs = 1.279(Pred) + 5.013$	.56
	7	$Obs = 1.781(Pred) - 0.560$	.68
N	3	$Obs = 0.358(Pred) + 0.835$	.86
	7	$Obs = 0.459(Pred) + 0.625$	.95
Cover	3	$Obs = 1.117(Pred) + 0.056$	.75
	7	$Obs = 1.033(Pred) + 0.309$	.75
G	3	$Obs = 0.741(Pred) + 20.396$	.88
X_0	3	$Obs = 1.251(Pred) + 23.330$	.99

We also ran the model holding the stand parameters h/R and C_{R^2} constant for all stands (we chose intermediate values from among those measured in the field) and predicted R^2 and N, to test the sensitivity of the model to these parameters. Table V shows the results for constant values of h/R and C_{R^2}. There is little change in the predicted values of R^2 and N, no systematic error caused by holding the stand variables constant, and no change in the rank order of observed and predicted values.

Table V. Model Results for Constant h/R (=1) and C_{R^2}(=.5)
(Band 3; G, X_0, S, and $V(S)$ same as in Table 3)

Site	R^2_{obs}	R^2_{pred}	N_{obs}	N_{pred}	C_{obs}	C_{pred}	%
15	14.04	4.86	6.42	21.95	.31	.37	84
20	10.62	3.15	15.57	36.35	.58	.40	69
1	13.86	13.14	3.73	3.91	.18	.18	100
2	16.02	13.59	2.48	4.74	.14	.22	64
3	18.18	15.93	3.58	5.35	.23	.30	77
4N	45.63	19.63	1.59	3.84	.25	.26	96
4S	24.21	9.18	1.55	5.98	.13	.19	68

6. DISCUSSION

Using the Li-Strahler simple variance-dependent canopy model, characterizing tree geometry, spatial and size distribution from field data, and deriving spectral data from TM imagery, we were able to predict tree cover in test sites with reasonable accuracy (80 to 100 percent using TM Band 7, 60 to 100 percent using TM Band 3). The model easily separates low from high density stands; rank order of observed and predicted cover values are similar.

The model is relatively insensitive to the stand parameters Γ (which predicts the amount of tree crown and associated shadow from the geometry of the trees), and C_{R^2} (the variance in tree size) as shown by the results using a standard value for h/R (from which Γ is calculated) and C_{R^2}. This mean that reasonable values for h/R and C_{R^2} can be chosen for a species or woodland type, and extended over large areas.

In this test, the model underestimates crown size and overestimates density in all sites. The correlations between observed and predicted values shows that density is predicted better that crown size. The problem appears to be that our technique for choosing component signatures overestimates the brightness of G, to which the model is very sensitive, and in most cases underestimates the brightness of X_0. However, regressions of observed and predicted G and X_0 values show very good correlation ($r^2 > .85$), so it may be possible to adjust values of G and X_0 from training data by simple regression. Another alternative is to predict G and X_0 using the model itself in test sites where size and density are known, and then extrapolate these signatures to other areas. This was tested in Sites 4N and 4S, with greatly improved predicted values of N and R^2.

7. CONCLUSIONS

The Li-Strahler canopy model provides a physically-based model which explains the major characteristics of reflectance, and variance in reflectance, in a sparsely wooded landscape in terms of variations in tree size and density, and shadowing geometry. This gives a functional explanation for the observed empirical relationship between reflectance (brightness) and tree cover.

As a technique, this model is most useful when it can be parameterized and run over large areas. Therefore, it needs to be tested further in the following ways. Sites need to be divided into "train" and "test" portions, to see if signature and parameter extension is possible. More sites, over a greater range of crown size and density, need to be included. The accuracy of predicted N and R^2 should be improved by averaging predictions from uncorrelated spectral bands, principal components, or multi-date imagery, and this must be tested. Further, this technique is most cost-effective when applied to the coarsest spatial resolution for which inter-pixel variance is sufficient to invert the model. This can be tested with lower resolution imagery, or by resampling TM to simulate lower resolution imagery. Finally, our field work this year has convinced us that an ellipsoid is a better shape model than a hemisphere in this landscape, and in future work, Γ will be calculated accordingly.

8. ACKNOWLEDGEMENTS

This work would not have been possible without the scientific and logistic support of Pierre Hiernaux and the personnel at ILCA/Mali, and Chris Justice and the GIMMS personnel, research authorization from the Ministère Education National, Mali, and the cooperation of the people in our study zones. We thank David Simonett, Dramane Dembélé, Dramane Diarra, Roy Cole and Moussa Traoré for field assistance. This work was supported by the National Aeronautics and Space Administration (NASA), Awards NAGW-788 and NGT 05010804.

9. REFERENCES

Franklin, J., "Thematic Mapper analysis of coniferous forest structure and composition," *International Journal Remote Sensing*, vol. 7, pp. 1287-1301, 1986.

Franklin, J. and A. Getis, "A second order analysis of the spatial pattern of Ponderosa pine," *American Association for the Advancement of Science, annual meeting*, Los Angeles, California, 1985.

Franklin, J., J. Michaelsen, and A. H. Strahler, "Spatial analysis of density dependent pattern in coniferous forest stands," *Vegetatio*, vol. 64, pp. 29-36, 1985.

Hiernaux, P., M. I. Cissé, and L. Diarra, "Bilan d'une saison d'es pluies 1984 tres deficitaire dans la Gourma (Sahel Malien). Première campagne de suivi et télédetection expérimentale, Annexe: Fiches descriptives des sites," Programme des Zones Aride et Semi-aride, Document du Programme, CIPEA, Bamako, Mali, 1984.

Hiernaux, P. and C. O. Justice, "Suivi du developpement vegetal au cours de l'ete 1984 dans le Sahel Malien," *International Journal of Remote Sensing*, 1986. In press.

Holben, B. N. and R. S. Fraser, "Effects of atmosphere and view illumination geometry on visible and near IR AVHRR radiance data," *International Journal of Remote Sensing*, vol. 5, pp. 145-160, 1984.

Horler, D. N. H. and F. J. Ahern, "Forestry information content of Thematic Mapper data," *International Journal of Remote Sensing*, vol. 7, pp. 405-428, 1986.

Justice, C. O., J. R. G. Townshend, B. N .Holben, and C. J .Tucker, "Analysis of the phenology of global vegetation using meteorological satellite data," *International Journal of Remote Sensing*, vol. 6, pp. 1271-1318, 1985.

Li, X., "Geometric-optical modeling of a conifer forest canopy," Ph.D. Dissertation, Department of Geography, University of California, Santa Barbara, CA, 1983.

Li, X. and A. H. Strahler, "Geometric-optical modeling of a conifer forest canopy," *IEEE Transactions on Geoscience and Remote Sensing*, vol. GE-23, pp. 705-721, 1985.

Logan, T. L. and A. H. Strahler, "Optimal Landsat transforms for forest applications," *Proceedings of the 16th International Symposium on Remote Sensing of Environment*, pp. 455-468, Ann Arbor, Michigan, 1982.

Strahler, A. H. and X. Li, "An invertible forest canopy reflectance model," *Proceedings of the Fifteenth International Symposium on Remote Sensing of Environment*, Environmental Research Institute of Michigan, Ann Arbor, 1981.

Tucker, C. J., J. R. G. Townshend, and T. E Goff, "African land-cover classification using satellite data," *Science*, vol. 277, pp. 369-375, 1985.

Tucker, C. J., C. Vanpraet, E. Boerwinkel, and A Gaston, "Satellite remote sensing of total dry matter production in the Senegalese Sahel," *Remote Sensing of Environment*, vol. 13, pp. 461-474, 1985.

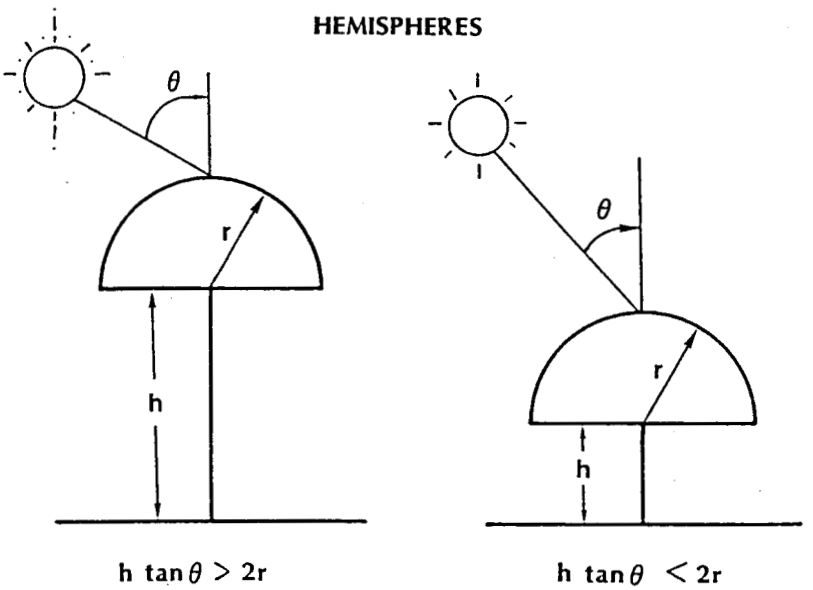

Figure 1. Tree form geometry.

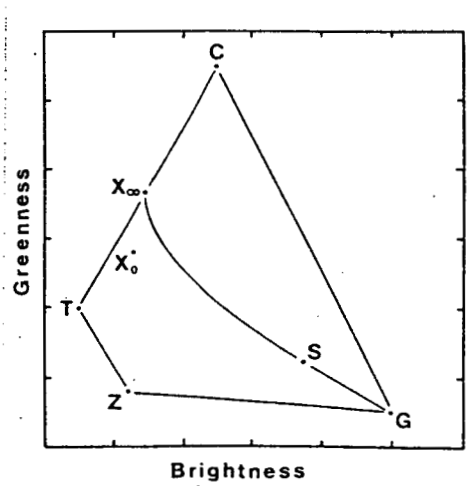

Figure 2. Idealized plot of model in multispectral space.

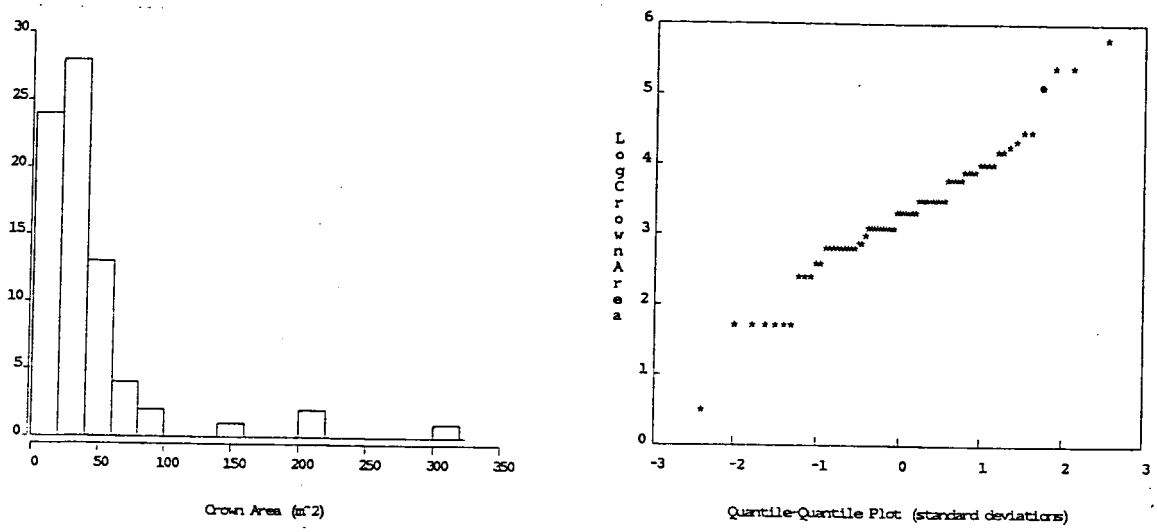

Figure 3. Size distribution of trees and Q-Q plot of log transform for Site 15.

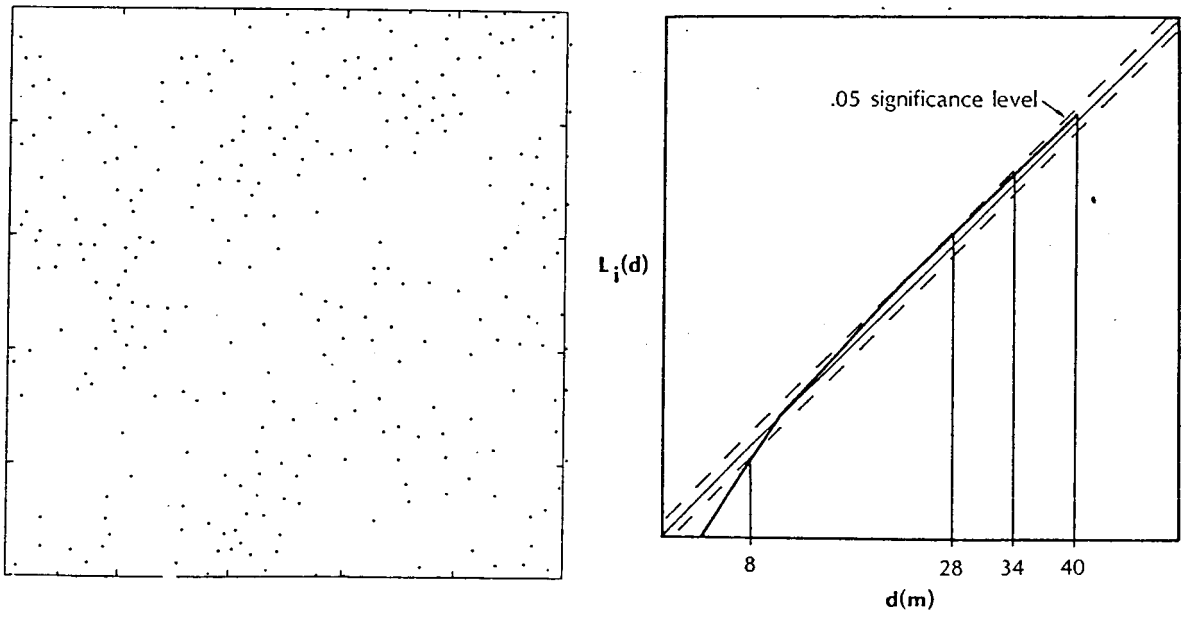

Figure 4. Point locations and results of second order analysis for Site 2.